



FLOODSTAND-deliverable:

**Report on validation and sensitivity testing of methods for
assessing effectiveness of abandonment process**

| | |
|-----------------|------------------------------------|
| Authors | P. MAURIER, Y. HIFI, Ph. CORRIGNAN |
| Organisation | Bureau Veritas, SSRC |
| Revision | 2 |
| Deliverable No. | D5.3 |

| | |
|------|------------------|
| Date | 23 December 2011 |
|------|------------------|



| Document identification sheet | |
|---|---|
| FLOODSTAND | Integrated Flooding Control and Standard for Stability and Crises Management |
| FP7-RTD- 218532 | |
| Title: Report on validation and sensitivity testing of methods for assessing effectiveness of abandonment process | Other report identifications: |
| Investigating partners: BV, SSRC Authors: P. MAURIER, Y. HIFI, Ph. CORRIGNAN Reviewed by: | |
| <input type="checkbox"/> Outline <input type="checkbox"/> Draft <input checked="" type="checkbox"/> Final Version number: 2 Revision date: Next version due: Number of pages: | <input checked="" type="checkbox"/> A deliverable <input type="checkbox"/> Part of a deliverable <input type="checkbox"/> Cover document for a part of a deliverable <input type="checkbox"/> Deliverable cover document <input type="checkbox"/> Other Deliverable number: 5.3 Work Package: 5 Deliverable due at month: 30 |
| Accessibility: <input checked="" type="checkbox"/> Public <input type="checkbox"/> Restricted <input type="checkbox"/> Confidential (consortium only) <input type="checkbox"/> Internal (accessibility defined for the final version) | Available from: http://floodstand.aalto.fi/ Distributed to: Discloses when restricted: Comments: |
| Abstract: This report present the main results achieved through the Task 5.3 of the FLOODSTAND project, entitled "Test/Develop abandonment (A) model". This task aims to develop requirements for a model describing the abandonment process, as a part of the MAR process described in the 5.1 deliverable of the FLOODSTAND project. Sensitivity analysis of the whole process (including the Abandonment process) was conducted in task 5.5 and presented in the deliverable 5.5. | |

Acknowledgements

The research leading to these results has received funding from the European Union's Seventh Framework Programme (FP7/2007-2013) under grant agreement n° 218532. The financial support is gratefully appreciated.

Disclaimer

Neither the European Commission nor any person acting on behalf of the FLOODSTAND Consortium is responsible for the use, which might be made of the following information. The views expressed in this report are those of the authors and do not necessarily reflect those of the European Commission and other members of the FLOODSTAND Consortium.

Copyright © 2010 FP7 FLOODSTAND project consortium

Reproduction is authorised provided the source is acknowledged

CONTENTS

| | Page |
|---|-------------|
| CONTENTS..... | 2 |
| 1. EXECUTIVE SUMMARY..... | 3 |
| 2. INTRODUCTION..... | 3 |
| 3. Part I: MAR process and list of obstacles..... | 4 |
| 4. PART II : THE ABANDONMENT PHASE..... | 6 |
| 4.1 Obstacles order and structure..... | 6 |
| 4.2 Obstacles selection..... | 7 |
| 5. Detailed description of obstacles..... | 8 |
| 5.1 Obstacle summary..... | 8 |
| 5.2 A1 - Deployment impossible..... | 8 |
| 5.3 A2 - Davit deployment failure..... | 9 |
| 5.4 A5 - Lifeboat engine failure..... | 11 |
| 5.5 A6 - Embarkation time..... | 11 |
| 5.5.1 The Estonia..... | 12 |
| 5.5.2 Cruise liner..... | 14 |
| 5.5.3 Time to board davit launched liferafts..... | 16 |
| 5.6 A7 - Structural failure/capsize due to premature release of the LSA..... | 18 |
| 5.7 A8 - Structural failure due to impacts of the LSA against the hull during lowering..... | 19 |
| 5.8 A9 - Injuries due to impacts of the LSA against the hull during lowering..... | 21 |
| 5.9 A10 - Injuries due to slamming..... | 23 |
| 5.10 A11 - Injuries while using the escape ladders..... | 24 |
| 5.11 A15 - Injuries while moving to seat..... | 26 |
| 5.12 A16 - Failure to clear off the vessel..... | 27 |
| 5.12.1 Lifeboats..... | 28 |
| 5.12.2 Liferafts..... | 30 |
| 6. Conclusions..... | 31 |
| 7. REFERENCES..... | 32 |
| A. Appendix A..... | I |
| B. Appendix B..... | XIX |

1. EXECUTIVE SUMMARY

This report presents the main results achieved through the Task 5.3 of the FLOODSTAND project, entitled “Test/Develop abandonment (A) model”. This task aims to develop requirements for a model describing the abandonment process, as a part of the MAR process described in the 5.1 deliverable of the FLOODSTAND project.

The whole process has been divided in several obstacles and each obstacle has then been evaluated. Specific models have been developed when needed and previous work from another European funded project has been exploited when relevant. For each obstacle, one or several obstacle matrices have been calculated.

According to the Description of Work, sensitivity testing was planned in each task from Task 5.2 to Task 5.4. However, it seems more meaningful to analyse the sensitivity of the expected number of fatalities at the end of the whole Mustering-Abandonment-Rescue process rather than on each phase individually. Consequently, it has been decided to conduct the sensitivity analysis in task 5.5 and present it in the deliverable 5.5.

2. INTRODUCTION

This deliverable is divided in two parts. The first part gives an overview of the Muster Abandonment and Rescue (MAR) process and the different obstacles that define it.

An introduction to the software developed to assess the overall process is presented in the deliverable 5.2 and its Appendix A.

In the second part the abandonment process is studied in detail and the results of the assessment of this phase are presented, each obstacle is evaluated and the corresponding matrices are described.

3. PART I: MAR PROCESS AND LIST OF OBSTACLES

As introduced in FLOODSTAND deliverable D5.1, the human health status (HHS) was chosen as the indicator to assess the risk for passengers when abandoning the ship.

The escape and rescue process (or route) was defined as a sequence of actions that passengers (and crew) need to perform in order to evacuate from their initial location to a place of safety (shore or rescuing vessel). In doing so, they would rely on Life Saving System (LSS).

Escape and rescue routes can be split up into four different phases as follows:

1. Mustering
2. Abandonment
3. Survival at sea
4. Rescue

In addition, the escape and rescue route can be defined as a series of obstacles which are characterised by the hazard they generate. These hazards can affect people directly (later referred to as Human Factor (HF) obstacle) or indirectly through the life saving appliances (later referred to as Hardware (HW) obstacles) by degrading (or not) their Health status.

So in order to define the Mustering, Abandonment and Rescue (MAR) process, the obstacles which constitute each phase needed to be identified.

Based on the findings of task 5.1 and the results of the FP6 funded project SAFECRAFTS, a first comprehensive list of obstacles for each phase of the process was produced. Then, a first review has been conducted to simplify this list and reduce it to a manageable size (for example there were 43 obstacles in the Mustering phase alone). The list of obstacles obtained after this review is presented hereafter.

In addition, during the assessment of the different obstacles, some of them were found to be less significant than previously thought. For example, obstacle A4 “Liferaft malfunction” was not relevant as Passenger ships, as a regulatory requirement (SOLAS), need to carry Life Saving Appliances (generally liferafts) in excess and the malfunction of a liferaft should not affect the spare LSA capacity. This allows to further simplify the list by ignoring some additional obstacles (shaded in the tables below).

Mustering

| Id | Obstacle | Type |
|-----------|---|-------------|
| M1 | Passengers' reaction time | N/A |
| M2 | Passengers' location | N/A |
| M3 | Passengers' (intrinsic) mobility | N/A |
| M4 | Effects of heel on passengers' mobility | N/A |
| M5 | Blocked doors | N/A |
| M6 | Objects obstructing the passage | N/A |
| M7 | Injuries due to the list (static) | HF |
| M8 | Injuries due to ship motions (dynamic) | HF |

Abandonment

| Id | Obstacle | Type |
|-----------|---|-------------|
| A1 | Deployment impossible | HW |
| A2 | Davit deployment failure | HW |
| A3 | Chute deployment failure | HW |
| A4 | Liferaft malfunction | HW |
| A5 | Lifeboat engine failure | HW |
| A6 | Embarkation time | |
| A7 | Structural failure/capsize due to premature release of the LSA | HW |
| A8 | Structural failure due to impacts of the LSA against the hull during lowering | HW |
| A9 | Injuries due to impacts of the LSA against the hull during lowering | HF |
| A10 | Injuries due to slamming | HF |
| A11 | Injuries while using the escape ladders | HF |
| A12 | Structural failure due to impact against the hull while afloat | HW |
| A13 | Injuries due to impact against the hull while afloat | HF |
| A14 | Failure of the bowsing lines | HW |
| A15 | Injuries while moving to seat | HF |
| A16 | Failure to clear off the vessel | HW |

Rescue

| Id | Obstacle | Type |
|-----------|---|-------------|
| R1 | Time to rescue passengers | N/A |
| R2 | Impossible to transfer passengers by using the side door | HW |
| R3 | Injuries while transferring passengers through the side door | HF |
| R4 | Impossible to transfer passengers by using the escape ladder, pilot ladder, rope ladder | HF |
| R5 | Injuries while transferring passengers with escape ladder, pilot ladder, rope ladder | HF |
| R6 | Capsizing/Downflooding | HW |
| R7 | Injuries due to LSA motions | HF |
| R8 | Hypothermia | HF |
| R9 | Seasickness | HF |

4. PART II : THE ABANDONMENT PHASE

The two reference ships selected by FLOODSTAND project have been evaluated. These ships have different means of escape:

- The Estonia, a ro-pax ship has 10 davit-launched lifeboat (LB) with a total capacity of 692 people and 63 liferafts (LR) with a total capacity of 1575 people. 12 LR are davit-launched and the others are boarded using escape ladder.
- The cruise liner has 18 davit-launched 150 people capacity lifeboats (LB) and 18 davit-launched 25 people capacity liferafts.

4.1 Obstacles order and structure

The following diagram shows the obstacle structure, the interactions between them and the order in which people pass through them depending on which type of LSA they will use. Availability parameters affect the number of LSA available for the following obstacles.

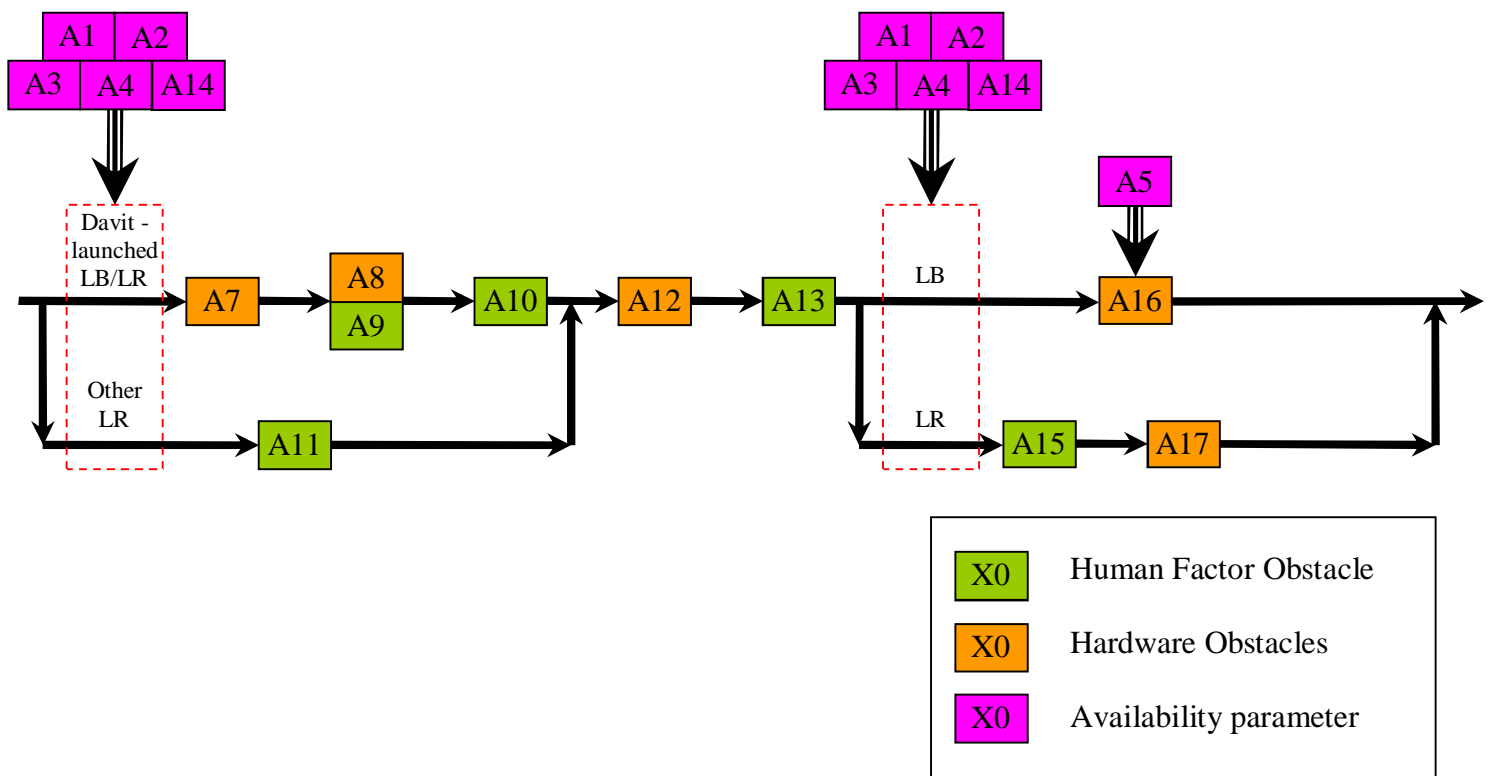


Figure 1 – Structure and order of obstacles

People pass through the obstacles from left to right, following the different paths depending on the means of rescue they are using (upper part in both branches if using a davit-launched lifeboat, upper then lower if using a davit-launched liferaft, lower in both branches if using the other type of liferaft).

Most of the obstacles of the abandonment phase have been previously studied in the FP6 funded project “*SAFECRAFTS: Safe abandoning of ships*”¹. As lifeboats and liferafts studied in this previous project are similar in their construction to those studied here it was agreed to exploit as much as possible the results of Safecrafts for the assessment of the above obstacles.

In the rest of the document a detailed description of the obstacles is provided as well as the assessment results.

4.2 Obstacles selection

As indicated in §3. , a comprehensive list of obstacles has been first established. Then this list has been reviewed in order to reduce the number of obstacles, as described hereafter.

Obstacle A3 (Chute deployment failure) was ignored as none of the ships considered in the project uses chutes (use of davit launched liferafts or liferafts boarded through ladder (Estonia)).

Obstacle A4 (Liferaft inflation failure) was also ignored as it was also assumed that there will be enough spare LSA and that losing some liferafts due to inflation failure would not have an impact.

From previous experience, obstacle A12 (Structural failure due to impact against the hull while afloat) and obstacle A13 (Injuries due to impact against the hull while afloat) were considered to have a small influence on the results, and to be negligible compared to “failure to clear off the vessel” (obstacle A16). Consequently, these obstacles were ignored.

The analysis of bowing lines performed in Safecrafts showed that no failure was to be expected. Consequently, the corresponding obstacle A14 has been ignored.

¹ <http://safecrafts.bal-pm.eu/>

5. DETAILED DESCRIPTION OF OBSTACLES

5.1 Obstacle summary

A short overview of each obstacle is given in a card as shown below. A brief explanation of each cell of the card can be found in the right column.

| | |
|--------------------------------|---|
| <i>Obstacle</i> | Number and name of the obstacle. |
| <i>Rescue route phase</i> | Phase in which the obstacle occur (Mustering, Abandonment or Rescue). |
| <i>Hardware / Human factor</i> | Type of obstacle Hardware or Human factor. |
| <i>Short Description</i> | A short description of the obstacle, how and when it appended during the phase. |
| <i>Parameter(s)</i> | A list of parameters influencing the results of the obstacle. |
| <i>Matrices to calculate</i> | Number of matrices to compute for this obstacle, given the input parameters. |
| <i>Model / Method</i> | A short description of the model or method used to calculate the obstacle. |
| <i>Results</i> | Short explanation of the results. |

5.2 A1 - Deployment impossible

| | |
|--------------------------------|---|
| <i>Obstacle</i> | A1 – Deployment impossible |
| <i>Rescue route phase</i> | Abandonment |
| <i>Hardware / Human factor</i> | Hardware |
| <i>Short Description</i> | The system cannot be deployed because of external conditions that might hamper its operability. Typically, large list angles higher than 20° may prevent the use of the system. |
| <i>Parameter(s)</i> | List |
| <i>Matrices to calculate</i> | One for each value of List considered. |
| <i>Model / Method</i> | No specific analysis has been performed to test the operability close to the boundary conditions as the system was deemed operable (within SOLAS requirement). |
| <i>Results</i> | No impact for all scenarios as system deemed operable. |

It was decided to use the regulatory limits. Above 20 degrees heel it is assumed that the lifeboats are not deployable (on the higher side of the ship), the number of lifeboats available for the abandonment phase is then reduced by the corresponding amount. Note : People that cannot use a lifeboat due to the reduced capacity will be assigned to a liferaft.

The degradation matrix for any list angle $\leq 20^\circ$ is then:

$$\begin{bmatrix} 1 & 0 & 0 & 0 \\ 0 & 1 & 0 & 0 \\ 0 & 0 & 1 & 0 \\ 0 & 0 & 0 & 1 \end{bmatrix}$$

5.3 A2 - Davit deployment failure

| | |
|--------------------------------|--|
| <i>Obstacle</i> | A2 – Davit deployment failure / malfunction |
| <i>Rescue route phase</i> | Abandonment |
| <i>Hardware / Human factor</i> | Hardware |
| <i>Short Description</i> | Different single failures may cause a malfunction of the davit deployment system: brake mechanism failure, davit mechanism failure, falls failure, winch failure are among the most significant. |
| <i>Parameter(s)</i> | None |
| <i>Matrices to calculate</i> | One |
| <i>Model / Method</i> | Results from Safecrafts (fault tree analysis performed) used for this obstacle. Applicable for both lifeboats and davit launched liferafts. |
| <i>Results</i> | Results are detailed below. |

Malfunction or failures during the deployment can have different causes. Based on historical data about occurrence of different failures covering a period of about 2 years and a half, the following basic faults were identified as being the most relevant in causing failure or malfunctioning during davit deployment:

- Brake mechanism
- Davit
- Falls

- Winch failure

These basic events were assumed independent and the “Malfunction” was assumed to occur as a result of at least one of these causes. As a result of this malfunction, we assume that everybody on the boat is lost.

A simple fault tree analysis was used to derive the overall probability of failure associated with the possible occurrence of one or several of these basic failures and was estimated to be 0.0032 (Figure 2).

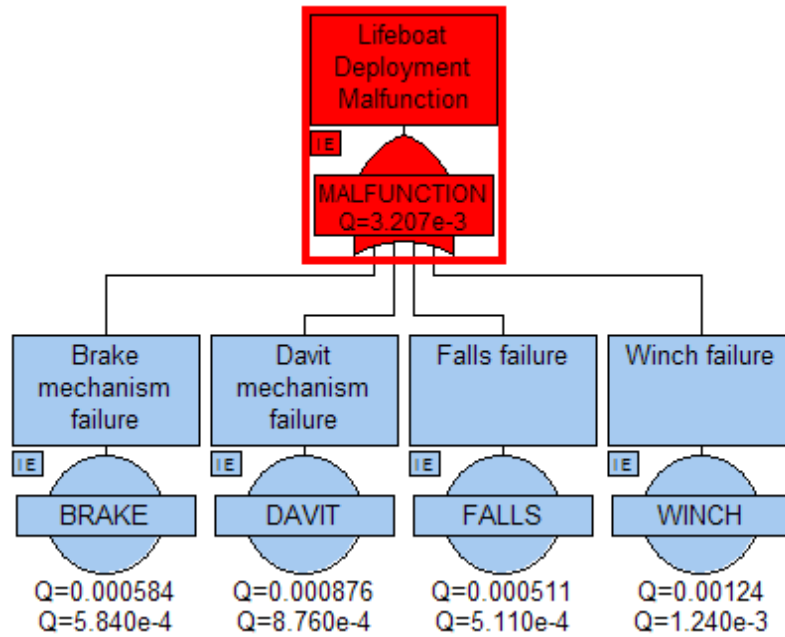


Figure 2: Fault tree for the obstacle deployment failure [ref Safecrafts]

Although this probability was initially estimated for lifeboat deployment malfunction, it is still valid here for liferafts as they are davit launched.

The degradation matrix associated with the obstacle is as follows:

$$\begin{bmatrix} 0.9968 & 0 & 0 & 0 \\ 0 & 0.9968 & 0 & 0 \\ 0 & 0 & 0.9968 & 0 \\ 0.0032 & 0.0032 & 0.0032 & 1 \end{bmatrix}$$

There is only one matrix for all scenarios.

In addition, the above calculations are considered to be generic and no distinction has been made between the different equipment types (different manufacturers) so for the case study the same matrix will be used for both the Estonia and the Cruise Liner.

5.4 A5 - Lifeboat engine failure

| | |
|--------------------------------|---|
| <i>Obstacle</i> | A5 – Lifeboat engine failure |
| <i>Rescue route phase</i> | Abandonment |
| <i>Hardware / Human factor</i> | Hardware |
| <i>Short Description</i> | A failure may occur when starting the engine. |
| <i>Parameter(s)</i> | None |
| <i>Matrices to calculate</i> | One |
| <i>Model / Method</i> | Results from Safecrafts used for this obstacle. Historical data from cruise industry and generic failure rates (based on historical data) taken from the offshore industry. |
| <i>Results</i> | Results are detailed below. This obstacle will be considered in conjunction with obstacle A16 below. |

The engine failure rate was estimated to be 0.01 based on data from the Offshore industry for which the range of the failure rate was established to be 1E-3 to 6E-2.

This obstacle is not scenario dependant so there is only one failure rate.

This obstacle is considered in conjunction with obstacle A16 below.

5.5 A6 - Embarkation time

| | |
|--------------------------------|---|
| <i>Obstacle</i> | A6 – Embarkation time |
| <i>Rescue route phase</i> | Abandonment |
| <i>Hardware / Human factor</i> | Hardware |
| <i>Short Description</i> | Time needed to embark the life saving appliances from muster stations |
| <i>Parameter(s)</i> | List. Three different heeling angles were considered 10°, 15° and 20°. |
| <i>Matrices to calculate</i> | No degradation matrices are calculated for this obstacle |
| <i>Model / Method</i> | Evacuation simulation software Evi used to assess the embarkation time. |

| | |
|----------------|---|
| <i>Results</i> | Different time of embarkation of LSA for the ships considered in the project. |
|----------------|---|

The embarkation of the LSA was modelled using Evi (please refer to D5.2 for a detailed description of Evi).

The required number of LSA to accommodate the total number of people on board is modelled.

The internal geometry of the lifeboats is not modelled.

The time needed by people to find a seat in the lifeboat or liferaft is modelled by controlling the flow rate at the door of the LSA.

The time to fill one lifeboat is based on Safecrafts data. According to tests done by the manufacturer a 150 people lifeboat was filled in 5 minutes. The flow rates at the lifeboats door were adjusted to reflect this.

The following assumptions are made:

- Embarkation starts once everybody has reached their muster station. Passengers and crew start from their assigned muster stations and proceed to the lifeboats and liferafts.
- LSA are ready for embarkation at the start of the simulation.
- LSA on both sides of the ship are available when the ship is heeling (within regulatory limits).
- Davit launched liferafts have the same filling rate as the lifeboats.

Simulations were performed for the following list angles (remain within the regulatory limits): 0°, 10°, 15° and 20°.

A description for each ship, of the location of people on board, life saving appliances, location of muster stations and the results of the embarkation simulation are presented below.

5.5.1 *The Estonia*

There were 10 motor-driven open lifeboats. The five boats on the port side were approved for a total of 368 people and the five on the starboard side for a total of 324 people.

There were also 63 inflatable rafts, approved for a total of 1575 people. They were stowed on decks 7 and 8 and were equipped with hydrostatic release mechanisms. Twelve rafts (four on deck 7) were equipped to be launched by davits. The remaining rafts were intended to be dropped into the sea.

All LSA are boarded from deck7.

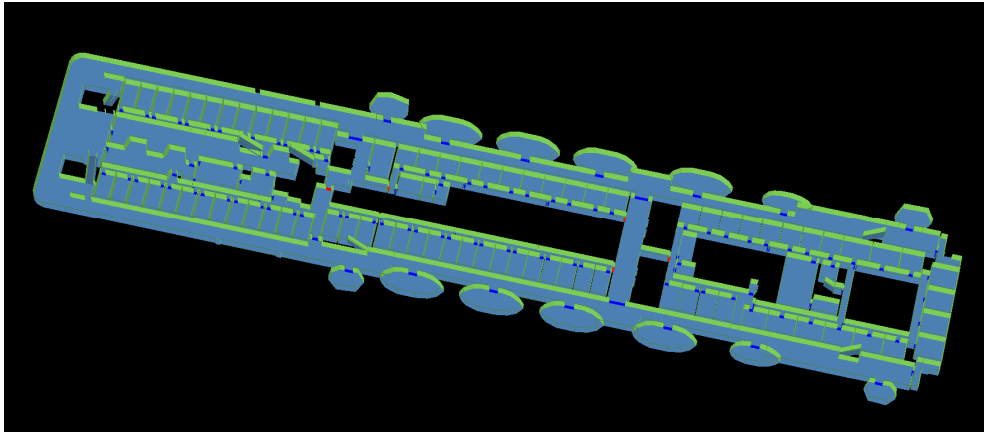


Figure 3: Evi model of the Embarkation deck of the Estonia

For the embarkation simulation the same number of people on board as the night of the accident was used i.e. 989.

We assume that all lifeboats will be used to full capacity which will accommodate 692 people. The remaining people i.e. 297 are assumed to use liferafts. To accommodate this number twelve liferafts are needed. Four of them are davit launched. The rest are dropped to the sea and are boarded from deck 7 using ladders.

The ladders were modelled by stairs of 0.7m width.

Liferafts at the sea surface were modelled at a distance of 1m of the mother ship's hull. For each embarkation station, there are two liferafts at sea connected to each other through a door (see Figure 4).

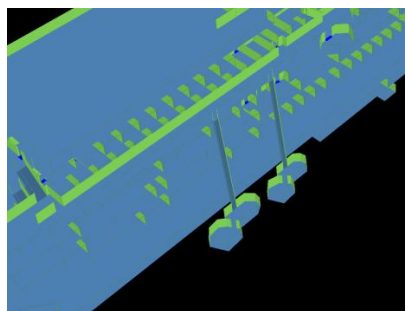


Figure 4: Evi model of the dropped liferafts and the ladder to board them

Accurate data about time to climb down the ladder are not available. Consequently, an average of 1 person every 40 seconds was used in the simulation.

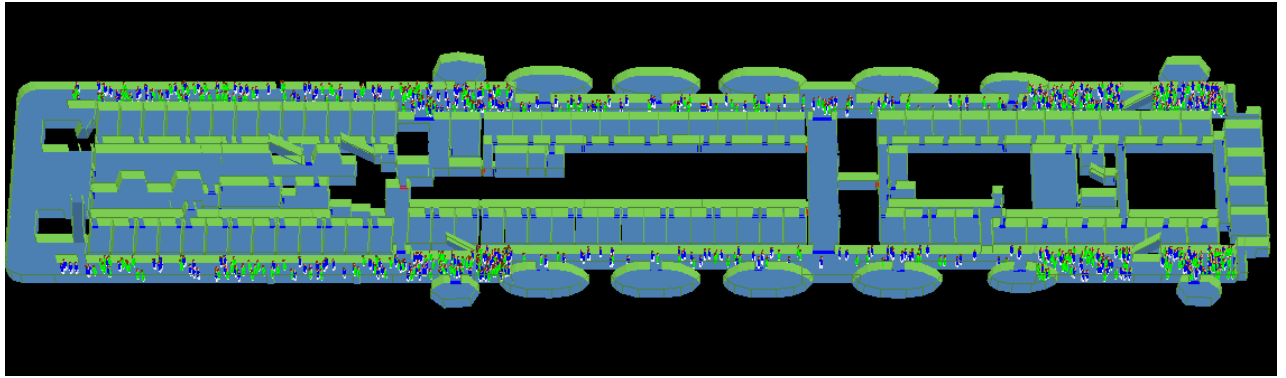


Figure 5: Passengers and crew location before embarkation

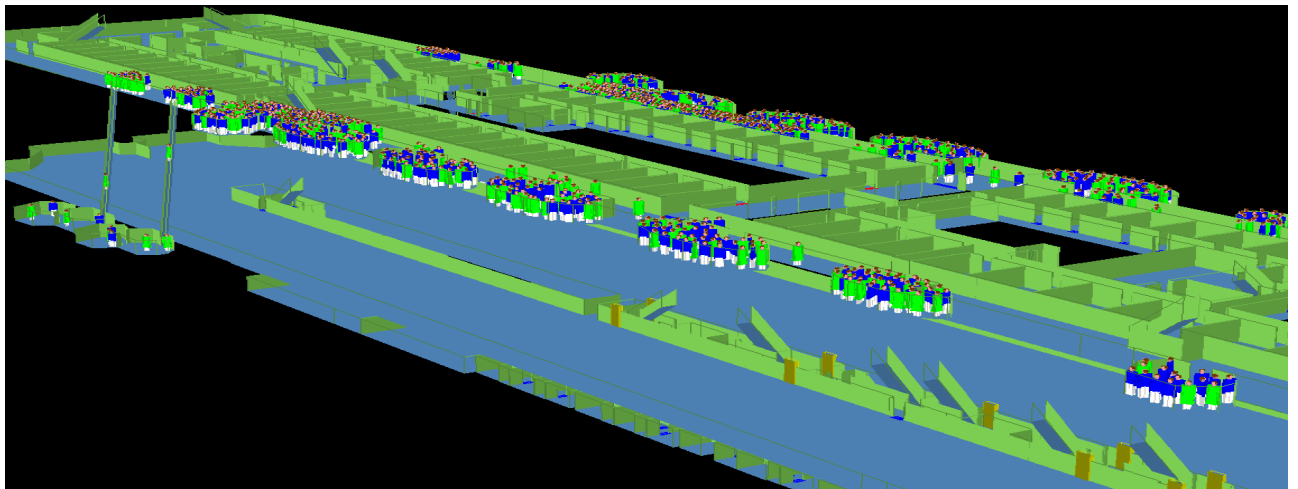


Figure 6: People embarking lifeboats and liferafts

The average embarkation time for 50 runs for different heel angles are shown in the table below:

| | | Heel angles (°) | | | |
|-------------|---------|-----------------|----|----|-----|
| | | 0 | 10 | 15 | 20 |
| Time (m) | Average | 34 | 34 | 35 | 51 |
| | Max | 47 | 54 | 57 | 101 |
| | Min | 28 | 29 | 28 | 29 |

5.5.2 Cruise liner

On both sides of the ship there are nine 150 person motor lifeboats as well as a rescue boat. There are also on each side of the ship 5 davit launched inflatable rafts aft and 13 fore. All liferafts have a 25 person capacity.

The embarkation deck is deck 7.

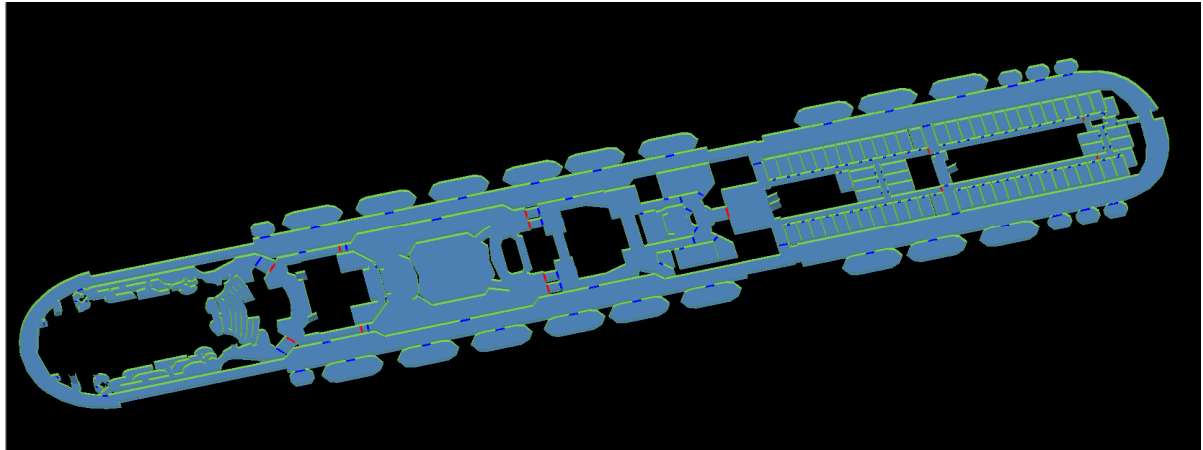


Figure 7: Embarkation deck of the cruise liner

The total number of people on board is 3388.

We assume that all 2557 passengers will abandon in lifeboats and the 831 crew members will abandon in liferafts. Although with this total number of passengers on board, a capacity of 143 seats remains available in lifeboats, this was not used to accommodate crew members. In real situations this may not be the case.

We also assume that only davit launched liferafts were used to accommodate the crew, which requires 29 liferafts.

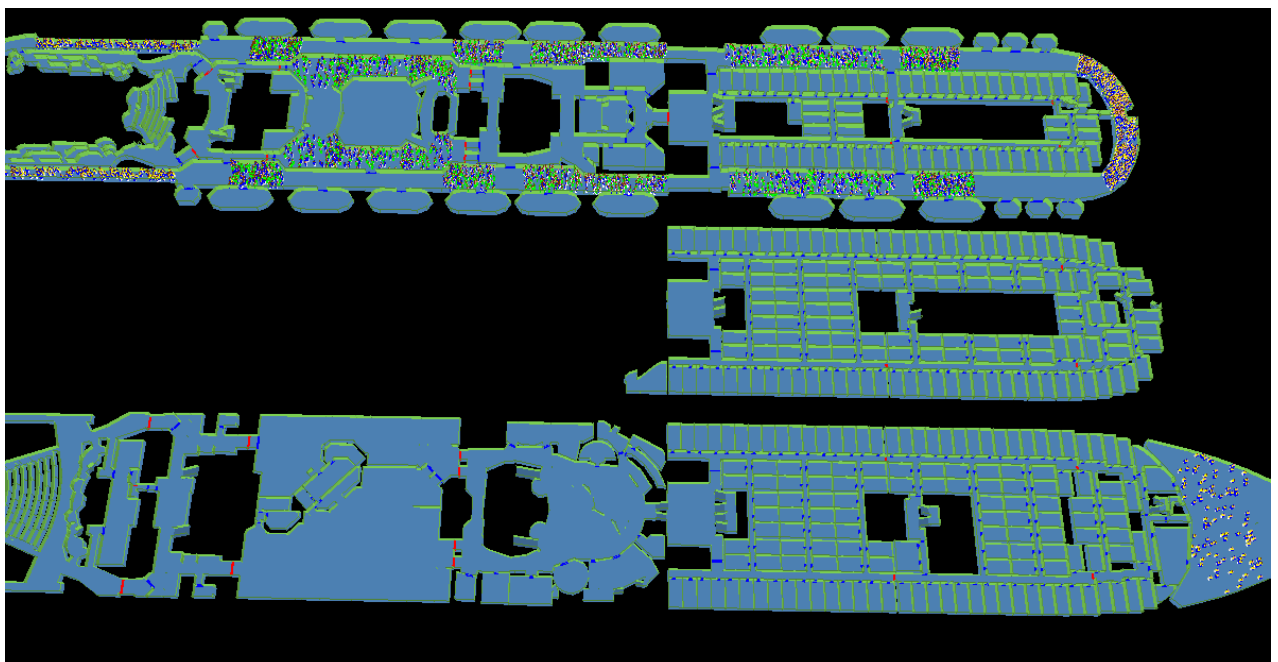


Figure 8: Initial location of passengers and crew before embarkation

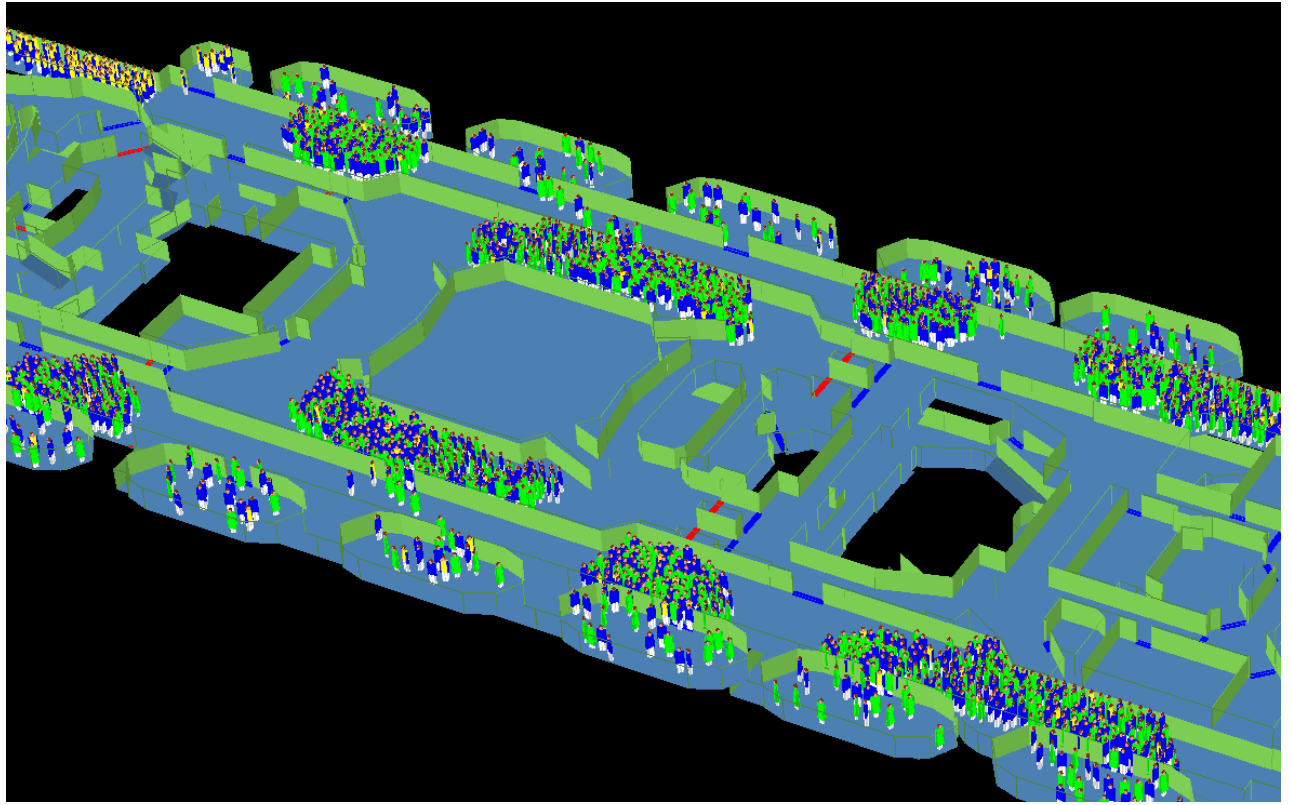


Figure 9: LSA embarkation for the cruise liner

5.5.3 Time to board davit launched liferafts

All lifeboats can be boarded at the same time but only 8 (4 on each side: 3 fore and 1 aft) davit launched liferafts can be boarded simultaneously, so the total embarkation time will depend on the time needed to board all the davit launched liferafts.

Davit launched liferafts have a capacity of 25 persons, so only $8 \cdot 25 = 200$ crew members can embark the liferafts at the same time. The remaining crew will need to wait for the previous liferafts to be filled, lowered and released from the hook. Then once the hook is retrieved the next liferafts need to be prepared (deployed, lowered and secured to the deck) before being ready to embark people.

We assume that liferafts that are boarded simultaneously are prepared in parallel.

The waiting time can be computed as follows:

$$t_{wait} = t_{prep} + t_{fill} + t_{lower} + t_{release}$$

Data for lifeboat preparation [ref RP490] in an evacuation exercise gave a measured time of 5 minutes and 30 seconds for the lifeboats to be ready for embarkation. In addition if we assume that liferaft inflation takes 2 minutes to 2 minutes and 30

seconds² then the total preparation time for davit launched liferafts is about 8 minutes. Assuming a conservative approach we can estimate that $t_{prep} t_{prep}$ is 10 minutes³.

$t_{fill} t_{fill}$ was estimated by Evi. Simulations (100 runs) of boarding a 25 persons davit launched liferaft gave an average time of 47 seconds.

$t_{lower} = h/v t_{lower} = h/v$, where:

- $v = 0.4 + 0.02hv = 0.4 + 0.02h$ (m/s) is the lowering speed of the liferaft which is assumed to be the same as for a lifeboat (IMO resolution A521 (13)) and
- h is the height (in meters) of the deck from which the LSA is lowered.

$t_{lower} t_{lower}$ was computed for different list angles for the highest side. Results are shown in the table below:

| Heel (°) | $t_{lower} t_{lower}$ (seconds) |
|----------|------------------------------------|
| 0 | 23 |
| 10 | 26 |
| 15 | 27 |
| 20 | 30 |

$t_{release} t_{release}$ which is the time to release and retrieve the hook was assumed to be 2 minutes.

There are 4 Crew muster stations. The number of crew members assigned to them and the number of davit liferafts needed to accommodate the crew are summarized in the table below:

| Muster station | # crew in muster stations | # DL_LR* |
|-----------------------------|---------------------------|------------------------|
| Aft port side (deck7) | 125 | 3 x 25 |
| Aft port side (deck7) | 125 | 3 x 25 |
| Fore (deck7) + Fore (deck5) | 369 + 100 | 9 x 25 PS + 10 x 25 SB |

* DL_LR ; Davit Launched Liferafts.

At the embarkation station 3 liferafts can be deployed and boarded at the same time.

For the first set of liferafts (at the beginning of the embarkation simulation) we assume that the liferafts are ready to embark i.e. $t_{prep} = 0 t_{prep} = 0$

The results of 50 simulation runs of the embarkation times (including preparation, filling the liferafts, lowering and releasing) for the different heel angles are summarized in the table below:

² Video on the web inflation of 25 person Viking LR: <http://www.youtube.com/watch?v=tBniOxAzoqY&feature=related>

³ Video davit launched LR on board drill rig : <http://www.youtube.com/watch?v=oU59HeeXPjs>

| | | Heel angles (°) | | | |
|----------|---------|-----------------|-------|-------|-------|
| | | 0 | 10 | 15 | 20 |
| Time (m) | Average | 53.65 | 54.00 | 53.97 | 54.06 |
| | Max | 56.55 | 56.28 | 55.07 | 55.80 |
| | Min | 52.79 | 53.05 | 53.20 | 53.35 |

The embarkation times are roughly the same whatever the heel angle as this is mainly due to the fact that no speed reduction occurs at these heel angles and the only difference is the lowering time which varies only by few seconds when the heel angle increases.

5.6 A7 - Structural failure/capsize due to premature release of the LSA

| | |
|--------------------------------|--|
| <i>Obstacle</i> | A7 – Structural failure / capsize due to premature release of the LSA |
| <i>Rescue route phase</i> | Abandonment |
| <i>Hardware / Human factor</i> | Hardware |
| <i>Short Description</i> | Davit-launched life saving appliances may experience failure of the hook that may cause unexpected release of the LSA. The lifeboat is then very likely to either have its structure damaged or capsize when falling violently into the sea. |
| <i>Parameter(s)</i> | None |
| <i>Matrices to calculate</i> | One |
| <i>Model / Method</i> | Results from Safecrafts used for this obstacle. |
| <i>Results</i> | Results are detailed below. |

Premature release of the LSA was mainly attributed to problems with on load hook. Although there are different designs for this type of hook, only the one considered the most dangerous (the “flat contact area cam” hook) was studied.

In a conservative approach it was assumed that the system studied was equipped with this type of hook.

The Probability of Premature release for the on load hook was estimated to be 0.0011.

This obstacle is not scenario dependent, so there is only one degradation matrix:

$$\begin{bmatrix} 0.9989 & 0 & 0 & 0 \\ 0 & 0.9989 & 0 & 0 \\ 0 & 0 & 0.9989 & 0 \\ 0.0011 & 0.0011 & 0.0011 & 1 \end{bmatrix}$$

5.7 A8 - Structural failure due to impacts of the LSA against the hull during lowering

| | |
|--------------------------------|---|
| <i>Obstacle</i> | A8 – Structural failure due to impacts of the LSA against the hull during lowering |
| <i>Rescue route phase</i> | Abandonment |
| <i>Hardware / Human factor</i> | Hardware |
| <i>Short Description</i> | Pendulum effect during lowering of the davit launched LSA due to the mother ship rolling, may result in impacts of the LSA against the mother ship’s hull and cause structural damage to the LSA. |
| <i>Parameter(s)</i> | Seas state (Hs), ship heading |
| <i>Matrices to calculate</i> | Three |
| <i>Model / Method</i> | Predictions of relative motions using time domain simulation coupled with a cable-body dynamics model. |
| <i>Results</i> | Results are detailed below. |

For the assessment of this obstacle it was decided to use data from a previous simulation study of lowering and recovery of a lifeboat available at SSRC (see Appendix A for a description of the initial study).

Although SSRC’s simulation was performed for sea state 6 (Hs=5m), it was considered that the results could be used as an upper limit or a worst case.

In the study different headings of the mother ship (0, 15, 30, 45, 60, 75, 90, 105, 120, 135, 150, 165 and 180 degrees) were considered.

The ship used in the study is roughly the same size as the Estonia. For the cruise liner which is a bigger ship the motion is assumed to be more moderate. So the data below would represent a worst case scenario for the cruise liner.

The predictions of relative motions have been performed using P R O T E U S 3, a time-domain mathematical model of ship responses in random seas, coupled with a cable-body dynamics model.

It has been assumed that the launching and recovery operations are carried out continuously. The deployment starts with a set speed of 30 m/min until the lifeboat reaches the calm water level, then it is immediately assumed to be recovered. When it reaches the initial deployment position again, it starts another launching operation.

The effect of collision has been ignored, in that the pendulation continues theoretically despite the physical contact between the lifeboat and the ship.

200 pendulum cycles have been simulated.

Simulations were performed for a ship in intact conditions. In damage situations, it is assumed that the motions would be less (damping).

The primary results of the study were the time series of the absolute mother ship and lifeboat motions, with the calculated relative distance between the sides of the lifeboat and the mother ship.

In order to use these results in the assessment of the obstacle A8, first for each heading the impacts and their numbers were identified then the velocity was calculated at each impact point.

We assumed that a structural failure would occur if the velocity at the impact exceeded 3.5m/s.

We obtained the following results:

- For 0° to 45° and 135° heading no impact was observed.
- For 60° heading only one impact was recorded with an impact velocity of 1.35ms⁻¹.
- For the rest of the headings the number of recorded impacts as well as the probability of exceeding 3.5m/s is shown in the table below. The probabilities were estimated based on probability function fitted to the data.

| Heading (°) | Number of impacts | Probability of velocity to exceed 3.5m/s |
|--------------------|--------------------------|---|
| 75 | 35 | 0.08 |
| 90 | 157 | 0.14 |
| 105 | 47 | 1.8 E-4 |
| 120 | 13 | 5.8 E-6 |
| 150 | 2 | 1.4775 E-4 |
| 165 | 4 | 1.32E-3 |
| 180 | 6 | 0.018 |

In a conservative approach we consider the worst case (90° heading) for which the probability of structural failure of one lifeboat is 0.14. In this case the degradation matrix would be for sea state 6:

$$\begin{bmatrix} 0.986 & 0 & 0 & 0 \\ 0 & 0.986 & 0 & 0 \\ 0 & 0 & 0.986 & 0 \\ 0.014 & 0.014 & 0.014 & 1 \end{bmatrix}$$

For lower sea states it is expected that no structural failure of the lifeboat would happen. The degradation matrix is then:

$$\begin{bmatrix} 1 & 0 & 0 & 0 \\ 0 & 1 & 0 & 0 \\ 0 & 0 & 1 & 0 \\ 0 & 0 & 0 & 1 \end{bmatrix}$$

5.8 A9 - Injuries due to impacts of the LSA against the hull during lowering

| | |
|--------------------------------|---|
| <i>Obstacle</i> | A9 – Injuries due to impacts of the LSA against the hull during lowering |
| <i>Rescue route phase</i> | Abandonment |
| <i>Hardware / Human factor</i> | Human Factor |
| <i>Short Description</i> | Pendulum effect because of the ship rolling during the davit launched LSA lowering phase may result in impacts of the LSA against the ship’s hull which are likely to cause injuries of the davit-launched LSA’s passengers |
| <i>Parameter(s)</i> | List, Sea State |
| <i>Matrices to calculate</i> | One for each combination of parameters List and Sea State |
| <i>Model / Method</i> | The consequence of an impact on human health is assessed and the probability of impact is calculated using results from the previous obstacle. The obstacle is then calculated using Probability × Consequence. |
| <i>Results</i> | No injury is to be expected in all scenarios due to low accelerations obtained in the simulations. Example matrix: $\begin{bmatrix} 1 & 0 & 0 & 0 \\ 0 & 1 & 0 & 0 \\ 0 & 0 & 1 & 0 \\ 0 & 0 & 0 & 1 \end{bmatrix}$ |

Results from calculations done for the previous obstacle (§5.7 - Structural failure due to impacts of the LSA against the hull during lowering) are given in the Appendix A.

The number of impacts is given by the table below, this number correspond to 200 cycles.

| Heading (°) | Number of impacts | Probability of impact |
|-------------|-------------------|-----------------------|
| 0 | 0 | 0 |
| 15 | 0 | 0 |
| 30 | 0 | 0 |
| 45 | 0 | 0 |
| 60 | 1 | 0.005 |
| 75 | 35 | 0.175 |
| 90 | 157 | 0.785 |
| 105 | 47 | 0.235 |
| 120 | 13 | 0.065 |
| 135 | 0 | 0 |
| 150 | 2 | 0.01 |
| 165 | 4 | 0.02 |
| 180 | 6 | 0.03 |

According to Safecrafts analyses and data (Safecrafts annex to deliverable 3.1), possible consequences for people of accelerations due to LB impacts against the hull are bruises and scratches, sprain, dislocation; fractures and blunt injuries; whiplash-like injuries, fractures of the cervical spine, and brain contusion with seriousness increasing with age and for passengers with mobility limitations.

For a conservative (optimistic) estimate, Safecrafts has ignored all fatalities due to fractures of cervical spine and brain contusion. They assumed that the injuries do not affect the vital system. No bracing position was assumed as it is unrealistic that passengers will be warned when the impact is coming. This would have mitigated the consequences. Passengers wear a life-jacket that could protect the body from impact but no mitigation was assumed as no information is available. It was assumed that disabled passengers (MM = Moderate Mobility and PM = Poor Mobility) will have a higher injury risk because they are less able to anticipate or to keep clear in an adequate way.

Consequences of an impact of the lifeboat against the ship's hull as a function of age:

Table B5. Consequences of an impact against the ship's hull simplified (GH = good health, MI = moderately injured, SI = severely injured, D = deceased).

| Age (years) | Injury severity | | | | total |
|-------------|-----------------|-----|----|----|-------|
| | GH | MI | SI | D | |
| <50 | 70% | 30% | 0 | 0 | 100% |
| 50-75 | 41% | 55% | 4% | 0 | 100% |
| >75 | 20% | 75% | 4% | 1% | 100% |

Using an average probability of impact and the consequences in above table, the matrix of the obstacle can be determined using Probability × Consequence.

| Sea State 6 | | | | | | | | | | | |
|-------------|---|---|---|--------------|--------|---|---|---------|--------|--------|---|
| Young <50 | | | | Middle 50-75 | | | | Old >75 | | | |
| 0.9694 | 0 | 0 | 0 | 0.9399 | 0 | 0 | 0 | 0.9185 | 0 | 0 | 0 |
| 0.0306 | 1 | 0 | 0 | 0.0561 | 0.9937 | 0 | 0 | 0.0764 | 0.9937 | 0 | 0 |
| 0 | 0 | 1 | 0 | 0.0041 | 0.0051 | 1 | 0 | 0.0041 | 0.0051 | 0.9975 | 0 |
| 0 | 0 | 0 | 1 | 0 | 0 | 0 | 1 | 0.0010 | 0.0013 | 0.0025 | 1 |

For other sea states, in Safecrafts results no injury was expected. The degradation matrix is then:

$$\begin{bmatrix} 1 & 0 & 0 & 0 \\ 0 & 1 & 0 & 0 \\ 0 & 0 & 1 & 0 \\ 0 & 0 & 0 & 1 \end{bmatrix}$$

5.9 A10 - Injuries due to slamming

| | |
|--------------------------------|--|
| <i>Obstacle</i> | A10 – Injuries due to slamming |
| <i>Rescue route phase</i> | Abandonment |
| <i>Hardware / Human factor</i> | Human Factor |
| <i>Short Description</i> | During lowering of the davit-launched lifeboats and liferafts, violent impact of the hull with water may lead to injuries for passengers. |
| <i>Parameter(s)</i> | Sea State |
| <i>Matrices to calculate</i> | One for each Sea State |
| <i>Model / Method</i> | Impact accelerations calculated for each Sea State will be compared to the human tolerance to acceleration. |
| <i>Results</i> | Two models for impact acceleration have been considered but only the second,, based on free fall of the boat from wave height has an effect on health. |

Detailed calculations and matrices are developed in Appendix B.

5.10 A11 - Injuries while using the escape ladders

| | |
|--------------------------------|--|
| <i>Obstacle</i> | A11 – Injuries while using the escape ladders |
| <i>Rescue route phase</i> | Abandonment |
| <i>Hardware / Human factor</i> | Human Factor |
| <i>Short Description</i> | Human Factor: Some passengers may be injured and fall at sea when embarking the liferaft with an escape ladder because of ship motions, list angle and their intrinsic vulnerability |
| <i>Parameter(s)</i> | Sea State |
| <i>Matrices to calculate</i> | One for each Sea State |
| <i>Model / Method</i> | Literature and accident report review done in Safecrafts. |
| <i>Results</i> | Matrices for different sea states were calculated and are described below. |

Climbing down a ladder is considered as difficult as climbing up a ladder, thus the following reasoning is considered as valid for this case.

In calm weather, from experimental values based on volunteers (Steenbekkers and Beijsterveldt, 1998), we estimate that 5% of the elderly would fail to climb the ladder.

From accident review, the case of foundering of the Achille Lauro in 1994 gives a rough estimate of the casualties in moderate weather (sea state 2 later increasing to 3 perhaps 4). On the 200 people who volunteered to climb the ladder (mainly young people), two fell from it, one knocked unconscious, the other may have died two days later (the report is unclear). The proportion of falls in the young group (<50) is thus 1%.

In order to take into account the older groups of people, a multiplying factor is applied. For the 50-75 group, this factor is 1.25, and for the older group, this factor is set to 5.

Injuries resulting from a fall were considered to be equally moderate, severe or fatal. Thus a 3% fall probability results in 1% moderate injuries, 1% severe injuries and 1% deaths.

Sea state 1 to 4

| <50 | GH | MI | SI | D |
|-----|--------|--------|--------|---|
| GH | 0.9910 | 0 | 0 | 0 |
| MI | 0.0033 | 0.9925 | 0 | 0 |
| SI | 0.0033 | 0.0041 | 0.9926 | 0 |
| D | 0.0033 | 0.0041 | 0.0082 | 1 |

| 50-75 | GH | MI | SI | D |
|-------|--------|--------|--------|---|
| GH | 0.9888 | 0 | 0 | 0 |
| MI | 0.0041 | 0.9907 | 0 | 0 |
| SI | 0.0041 | 0.0051 | 0.9907 | 0 |
| D | 0.0041 | 0.0051 | 0.0102 | 1 |

| >75 | GH | MI | SI | D |
|-----|--------|--------|--------|---|
| GH | 0.9551 | 0 | 0 | 0 |
| MI | 0.0164 | 0.9632 | 0 | 0 |
| SI | 0.0164 | 0.0202 | 0.9638 | 0 |
| D | 0.0164 | 0.0202 | 0.0396 | 1 |

Sea state 5 and 6:

The proportion of falls for sea state 5 and 6 was raised to 2.4% for the young group.

| <50 | GH | MI | SI | D |
|-----|--------|--------|--------|---|
| GH | 0.9760 | 0 | 0 | 0 |
| MI | 0.0080 | 0.9802 | 0 | 0 |
| SI | 0.0080 | 0.0099 | 0.9804 | 0 |
| D | 0.0080 | 0.0099 | 0.0196 | 1 |

| 50-75 | GH | MI | SI | D |
|-------|--------|--------|--------|---|
| GH | 0.9702 | 0 | 0 | 0 |
| MI | 0.0099 | 0.9754 | 0 | 0 |
| SI | 0.0099 | 0.0123 | 0.9757 | 0 |
| D | 0.0099 | 0.0123 | 0.0243 | 1 |

| >75 | GH | MI | SI | D |
|-----|--------|--------|--------|---|
| GH | 0.8810 | 0 | 0 | 0 |
| MI | 0.0397 | 0.9047 | 0 | 0 |
| SI | 0.0397 | 0.0476 | 0.9093 | 0 |
| D | 0.0397 | 0.0476 | 0.0907 | 1 |

5.11 A15 - Injuries while moving to seat

| | |
|--------------------------------|--|
| <i>Obstacle</i> | A15 – Injuries while moving to seat |
| <i>Rescue route phase</i> | Abandonment |
| <i>Hardware / Human factor</i> | Human Factor |
| <i>Short Description</i> | Difficulty moving and getting seated in the liferafts: While walking or crawling to reach their seat passengers may fall because (a) they are old, (b) the floor is flexible and destabilising and (c) the floor can be wet. |
| <i>Parameter(s)</i> | Sea State |
| <i>Matrices to calculate</i> | One for each Sea State |
| <i>Model / Method</i> | Analysis, mainly based on expert opinion, performed in Safecrafts |
| <i>Results</i> | <p>Example matrix (Sea State 5, >75):</p> $\begin{bmatrix} 0.9800 & 0 & 0 & 0 \\ 0.0200 & 0.9300 & 0 & 0 \\ 0 & 0.0700 & 0.9800 & 0 \\ 0 & 0 & 0.0200 & 1 \end{bmatrix}$ |

From Safecrafts analysis, the consequence of falling is described as follows:

Table B3. Distribution of injury consequences given a fall when walking inside the raft (GH = good health, MI = moderately injured, SI = severely injured, D = deceased).

| | Injury severity | | | | total |
|---------------------|-----------------|-----|----|---|-------|
| | GH | MI | SI | D | |
| Age in years | | | | | |
| <50 | 99% | 1% | 0 | 0 | 100% |
| 50-75 | 98% | 2% | 0 | 0 | 100% |
| >75 | 90% | 10% | 0 | 0 | 100% |

The model needs the product probability x consequences (**P x C**).

The probability of falling as been discussed in Safecrafts and results in the following degradation matrices:

| Sea State 3 | | | | | | | | | | | |
|-------------|--------|---|---|--------------|--------|---|---|---------|--------|--------|---|
| Young <50 | | | | Middle 50-75 | | | | Old >75 | | | |
| 0.9990 | 0 | 0 | 0 | 0.9990 | 0 | 0 | 0 | 0.9800 | 0 | 0 | 0 |
| 0.0010 | 0.9990 | 0 | 0 | 0.0010 | 0.9990 | 0 | 0 | 0.0200 | 0.9980 | 0 | 0 |
| 0 | 0.0010 | 1 | 0 | 0 | 0.0010 | 1 | 0 | 0 | 0.0020 | 0.9990 | 0 |
| 0 | 0 | 0 | 1 | 0 | 0 | 0 | 1 | 0 | 0 | 0.0010 | 1 |

| Sea States 5 and 6 | | | | | | | | | | | |
|--------------------|--------|---|---|--------------|--------|--------|---|---------|--------|--------|---|
| Young <50 | | | | Middle 50-75 | | | | Old >75 | | | |
| 0.9990 | 0 | 0 | 0 | 0.9970 | 0 | 0 | 0 | 0.9800 | 0 | 0 | 0 |
| 0.0010 | 0.9500 | 0 | 0 | 0.0030 | 0.9300 | 0 | 0 | 0.0200 | 0.9000 | 0 | 0 |
| 0 | 0.0500 | 1 | 0 | 0 | 0.0700 | 0.9800 | 0 | 0 | 0.1000 | 0.9200 | 0 |
| 0 | 0 | 0 | 1 | 0 | 0 | 0.0200 | 1 | 0 | 0 | 0.0800 | 1 |

5.12 A16 - Failure to clear off the vessel

| | |
|--------------------------------|---|
| <i>Obstacle</i> | A16 – Failure to clear off the vessel |
| <i>Rescue route phase</i> | Abandonment |
| <i>Hardware / Human factor</i> | Hardware |
| <i>Short Description</i> | The LSA may not be able to clear off the vessel for different reasons: unsuitable propelling, lack of manoeuvrability, failure to release from hook, etc. |
| <i>Parameter(s)</i> | Sea state |
| <i>Matrices to calculate</i> | Two |
| <i>Model / Method</i> | Combination of different basic failures for lifeboats. Safecrafts results for liferafts. |
| <i>Results</i> | Results from Safecrafts used for this obstacle |

This obstacle will be assessed for both the lifeboats and liferafts.

5.12.1 Lifeboats

Lifeboats may not be able to clear off for different reasons. Based on the available data the following failures were identified as being causes for failure to clear off:

- failure of release from the falls
- failure of the engine
- manoeuvring capacity of the lifeboat

The release mechanism was found to be problematic and prevents the disconnection of the LSA from the launching appliance.

Historical data from cruise industry and failure rates from the offshore industry were used to give simple estimate for the failure of release as follows:

In calm weather conditions the failure rate is estimated to be 0.001. For moderate conditions it is 0.01 and in severe weather conditions it is 0.1.

The failure rate of the lifeboat engine was estimated to be 0.001 (see obstacle A5 above).

The manoeuvring capacity of the lifeboats was assessed through simulation for different wind speeds and directions, as shown in the table below. In high sea states it was assumed that lifeboats in the leeward side would always be able to drift away.

| | | Wind direction (deg) | | | | | | | |
|--------------------|----|----------------------|-------------------------|-------|-------------|-------|---------------|--------|---------------------------|
| | | Beam (sheltered) | Quarter bow (sheltered) | Head | Quarter bow | Beam | Quarter stern | Stern | Quarter stern (sheltered) |
| | | 0 | 45 | 90 | 135 | 180 | 225 | 270 | 315 |
| Wind speed (knots) | 15 | Green | Green | Green | Green | Green | Green | Green | Green |
| | 20 | Green | Green | Green | Green | Green | Green | Green | Green |
| | 25 | Green | Green | Green | Yellow | Green | Green | Green | Green |
| | 30 | Green | Green | Green | Yellow | Red | Yellow | Green | Green |
| | 35 | Green | Green | Green | Red | Red | Red | Green | Green |
| | 40 | Green | Green | Green | Red | Red | Red | Green | Green |
| | 45 | Green | Green | Green | Red | Red | Red | Yellow | Green |
| | 50 | Green | Green | Green | Red | Red | Red | Yellow | Green |

-  Lifeboat can clear away from the ship
-  Lifeboat cannot clear away from the ship
-  Lifeboat can clear away from the ship with difficulties

The probability of casting off is given by:

$$P_{casting_off} = \sum [(P)_{wind_direction} \times P_{clear_away}]$$

In order to compute the probability of a successful casting off we assume the following:

1. The different wind directions are equally likely so we have a probability of $P_{wind_direction} = 1/8$.
2. If the lifeboat can clear away from the ship (green colour in the table above) this translates into a probability of success of $P_{clear_away} = 0.99$ *
3. If the lifeboat can clear away from the ship with difficulties (yellow colour in the table) we can assume a probability of $P_{clear_away} = 0.5$ *
4. If the lifeboat cannot clear away from the ship (red colour) than we assume a probability of $P_{clear_away} = 0.01$ *

***Note:**

The values assigned to the probability of clearing away are estimate. The sensitivity of the model to these values is assessed in the Deliverable 5.5.

So the for the different sea states we have:

Below Sea state 3, we assume no manoeuvring difficulties so the probability of success is 1.

$$\text{Sea state 3 } P_{casting_off} = 0.99$$

$$\text{Sea state 5 } P_{casting_off} = 0.92875$$

$$\text{Sea state 6 } P_{casting_off} = 0.6225$$

The probability of clearing off is then (failure of engine, failure of release and manoeuvring are independent events):

$$P_{clearing} = (1 - P_{failure_engine}) \times (1 - P_{failure_release}) \times P_{casting_off}$$

The degradation matrices are then

Sea state 0-1

$$\begin{bmatrix} 0.998 & 0 & 0 & 0 \\ 0 & 0.998 & 0 & 0 \\ 0 & 0 & 0.998 & 0 \\ 0.002 & 0.002 & 0.002 & 1 \end{bmatrix}$$

Sea state 3

$$\begin{bmatrix} 0.979 & 0 & 0 & 0 \\ 0 & 0.979 & 0 & 0 \\ 0 & 0 & 0.979 & 0 \\ 0.021 & 0.021 & 0.021 & 1 \end{bmatrix}$$

Sea state 5

$$\begin{bmatrix} 0.835 & 0 & 0 & 0 \\ 0 & 0.835 & 0 & 0 \\ 0 & 0 & 0.835 & 0 \\ 0.165 & 0.165 & 0.165 & 1 \end{bmatrix}$$

Sea state 6

$$\begin{bmatrix} 0.560 & 0 & 0 & 0 \\ 0 & 0.560 & 0 & 0 \\ 0 & 0 & 0.560 & 0 \\ 0.440 & 0.440 & 0.440 & 1 \end{bmatrix}$$

5.12.2 Liferafts

It was found that up to sea state 3, it was possible to tow liferafts. So they would be able to clear off in those conditions.

In higher sea states it was assumed that liferafts in windward would be lost and the ones in the leeward side would drift.

So the degradation matrices are as follows:

Up to sea state 3

$$\begin{bmatrix} 1 & 0 & 0 & 0 \\ 0 & 1 & 0 & 0 \\ 0 & 0 & 1 & 0 \\ 0 & 0 & 0 & 1 \end{bmatrix}$$

Higher sea states

$$\begin{bmatrix} 0.5 & 0 & 0 & 0 \\ 0 & 0.5 & 0 & 0 \\ 0 & 0 & 0.5 & 0 \\ 0.5 & 0.5 & 0.5 & 1 \end{bmatrix}$$

6. CONCLUSIONS

The objective of WP5 is to develop models for the assessment of the risk to human associated with the whole Muster Abandonment and Rescue (MAR) process. The methodology developed in Task 5.1 to perform such an assessment is based on two concepts: a decomposition of the whole process into a succession of obstacles that people have to pass and the Human Health Status (HHS), which gives the proportion of people in Good Health / Minor Injury / Sever injury / Dead categories. The impact of passing a given obstacle on the health of people is translated by a modification of the HHS vector after the obstacle. This modification is calculated by multiplying the HHS vector before the obstacle by a “degradation” matrix, specifically determined for this obstacle.

In this context, and according to the Description of Work, Task 5.3 focused on the Abandonment phase of the MAR process. First, the obstacles relevant for the Abandonment phase have been identified, resulting in a list of 11 obstacles. Then, each obstacle has been analysed and the corresponding degradation matrix/matrices have been determined. These analyses and results are presented in this report.

The matrices have been input into the Casualty Calculator program (developed within Task 5.2 and described in D5.2).

The sensitivity analysis of the expected number of fatalities with the input parameters relevant to the Abandonment phase is included with the global sensitivity analysis performed in Task 5.5 and presented in Task 5.5.

7. REFERENCES

TNO Human Factors, Safecrafts Deliverable 3.1, *Passengers Health along the Rescue Route*, 2006

Louis Boer Consult, Safecrafts update to Deliverable 3.1, *The Rescue Route in terms of Passenger Health*, June 2007

Laurent PRAT (BV), Dr. Philippe CORRIGNAN (BV), Safecrafts Deliverable 4.2, *“Quantitative assessment of two existing rescue systems & Identification of critical areas”*. 2008

MCA Research project 490. Phase 1: the effect of ship motions on the evacuation process. *“Task3.1a: critical review of data available as input to evacuation simulation tools”*. SSRC 2004

Harris, C. M., & Bert, C. W. (2002). *Shock and Vibration Handbook (5th ed.)*. *Journal of Applied Mechanics*.

von Karman, T. (1929). *The Impact on Seaplane floats during landing*.

A. APPENDIX A

Objectives

The objective has been to assess operational conditions during launch and recovery of a RIB from a side of a ship while proceeding in a bow and stern-quartering long-crested waves. The operational conditions relate to expected amplitudes of relative motions in horizontal direction between sides of the ship and the RIB during deployment operation.

Approach adopted

The predictions of relative motions have been performed by using a *time-domain* mathematical model of ship responses in random seas, P R O T E U S 3, coupled with a cable-body dynamics model. The mathematical background is given in **Appendix 1**.

The sea conditions have been modelled by a JONSWAP sea spectrum, as described in **Appendix 2**, with the variable parameters given in the table below.

| | Significant Wave Height Hs [m] | Modal Period Tp [s] |
|-------------|--------------------------------|---------------------|
| Sea State 6 | 5.0 | 12.4 |

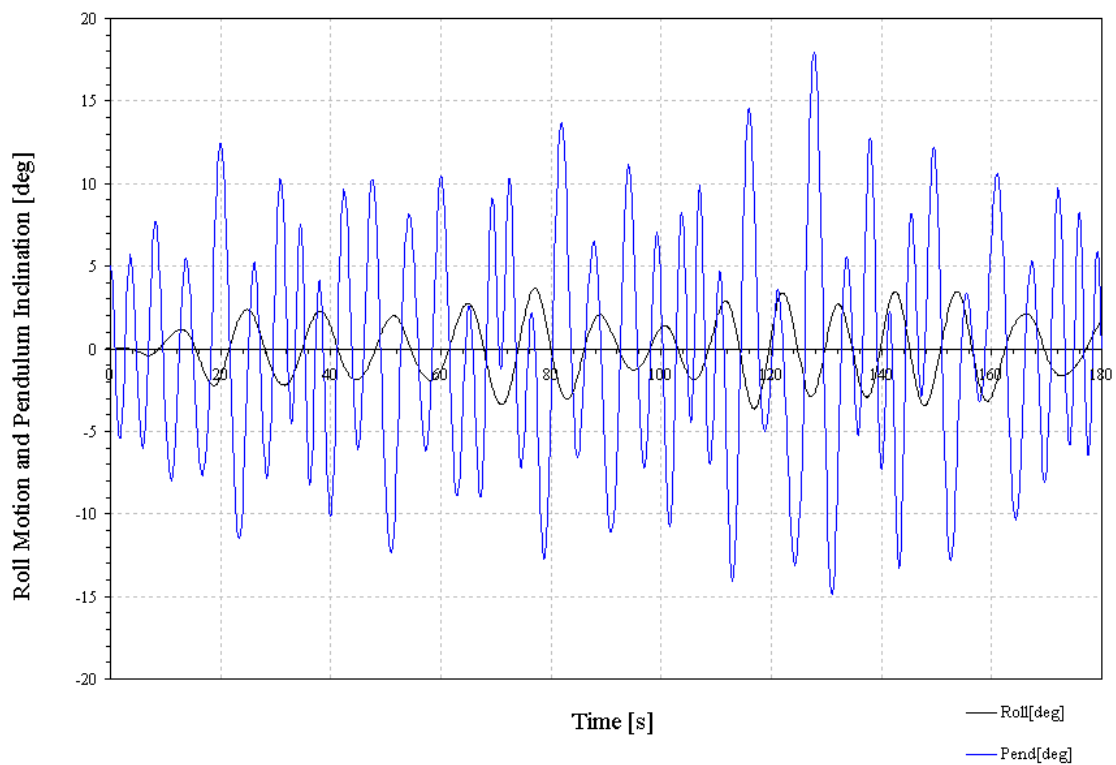
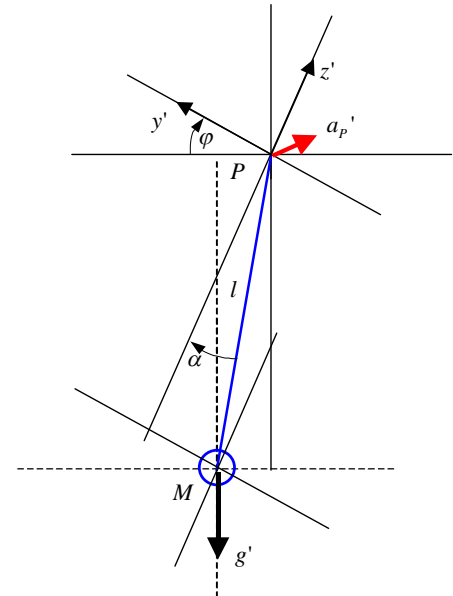
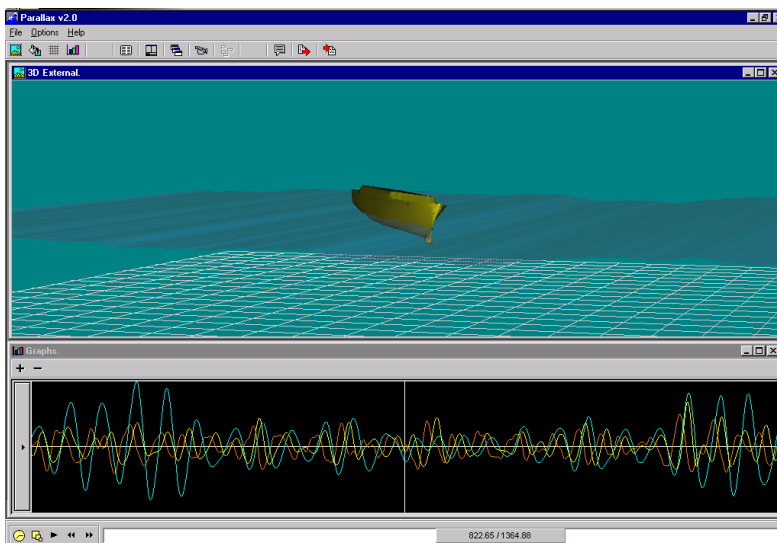
The ship motion prediction model has been subject to validation study by means of comparison of predictions with experimental measurements.

The boom tip point (attachment point of the RIB) is located 36m aft of the midship, 17.1m from the base plane and 13.35m to starboard side from the centre-plane. The least vertical distance between the boom tip and the centre of gravity (CG) of the RIB is 2.3m. The maximum vertical distance between the boom tip and the CG of the RIB has been assumed as 11.76m, which is when the RIB's CG attains calm water level. The RIB's breadth is 3.02m. The relative distance between the RIB's side and the ship side is estimated based on the profile of the ship hull at the RIB deployment location. The average speed of 30m/min for RIB launch/recovery has been assumed.

Predictions of ship motions and the pendulation

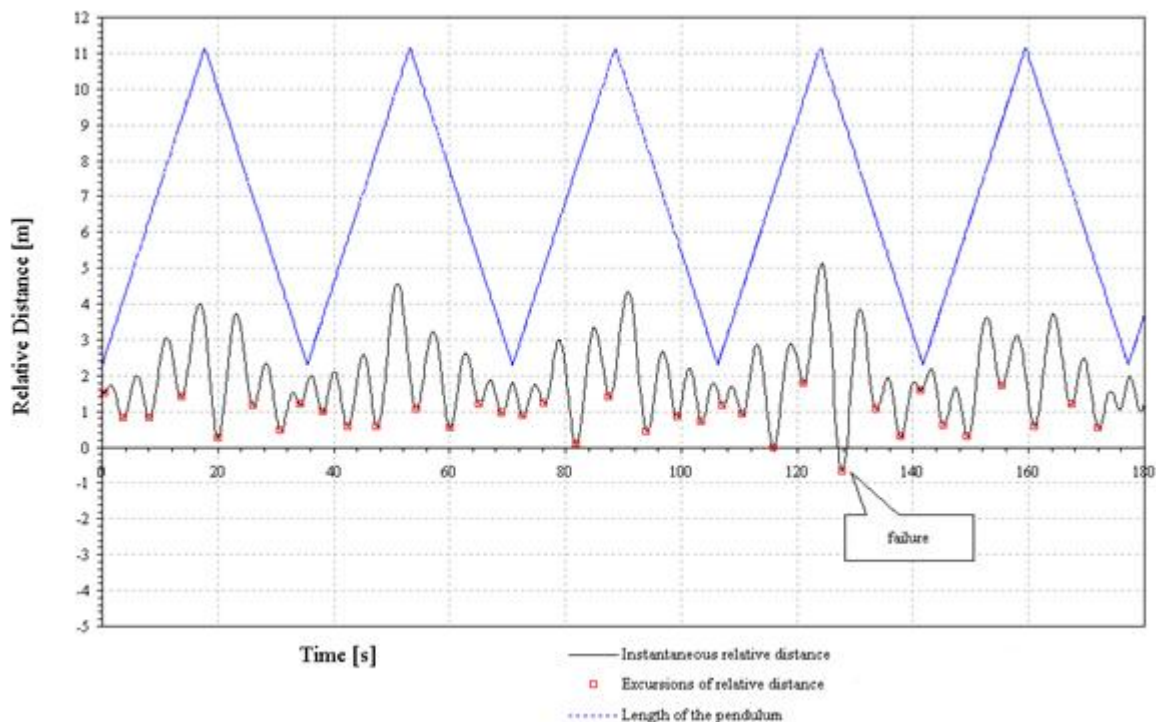
As mentioned above, the time domain simulation of ship motions and RIB pendulation, as it is lowered and recovered with constant speed, has been based on the P R O T E U S 3 software suit, coupled with cable body dynamics model. The simulations were performed for at least 1 hour duration for each single condition tested.

The eventual signal of interest is the time series of the instantaneous distance between sides of the RIB and the SHIP, which varies as a result of ship motions, RIB pendulation (affected by ship motion and the length of the sling while it is launched and recovered), and the profile of the SHIP varying with the vertical position of the RIB.



Statistical analyses of the excursions of relative distance between the RIB and the ship

The time series of the instantaneous distance between sides of the RIB and the ship is analysed in terms of its minimum amplitudes (excursions). The collision of RIB with the ship is considered when the relative distance is zero or less. The process of the relative motion between the RIB and the ship is a highly non-linear and non-stationary random process.



The above analyses have been performed for a series of 13 headings between 0-180deg.

Numerical results and discussions

The primary results of the investigation are the time series of the absolute ship and the RIB motions, with the calculated relative distance between the sides of the RIB and the ship.

General trends

It has been assumed that the operations are carried out continuously, that is the deployment starts with a set speed of 30 m/min until the RIB reaches the calm water level, and once this happens it immediately is assumed to be recovered. When it reaches the initial deployment position again, it commences another launching operation. Although the vertical conditions for each of these operations are always the same, the horizontal location of the RIB is always assumed to continue from the previous operation. In other words, if the RIB has just been launched to the calm water level, and the horizontal distance to the hull was 5m as a result of pendulum swinging, then the retrieval operation starts for RIB at this horizontal location. This assumption is well conditioned to also take into account the randomness of the conditions at the commencement of each operation, in particular retrieval. Although the assumption has some inherent conservatism, it has been accepted for the sake of (a) over-prediction of the probabilities of failure, thus leading to safer conclusions (b) expected actual low impact of the assumption on the predictions, on one hand, and (c) easier post-processing of the simulations on the other. Also the effect of collision has been ignored, in that the pendulation continues theoretically despite the physical contact between the RIB and the ship. This is also a conservative assumption leading to possibly overestimation of probabilities of failures.

From general considerations of the pendulation, it can be deduced that the conditions for resonant RIB response approach its worst in terms of amplitude of the response and the ensuing probabilities of failure of the operation, when the RIB is near the calm water surface. However, as is shown in Figure 10, the peak response at this position (11.76 m from the boom tip) occurring for periods just below 7s is still relatively far from the resonant periods of sea state 6 with modal period of 12.4 s. Therefore there is only moderate dynamic resonance effect, since the RIB is excited predominantly at sub-harmonic periods.

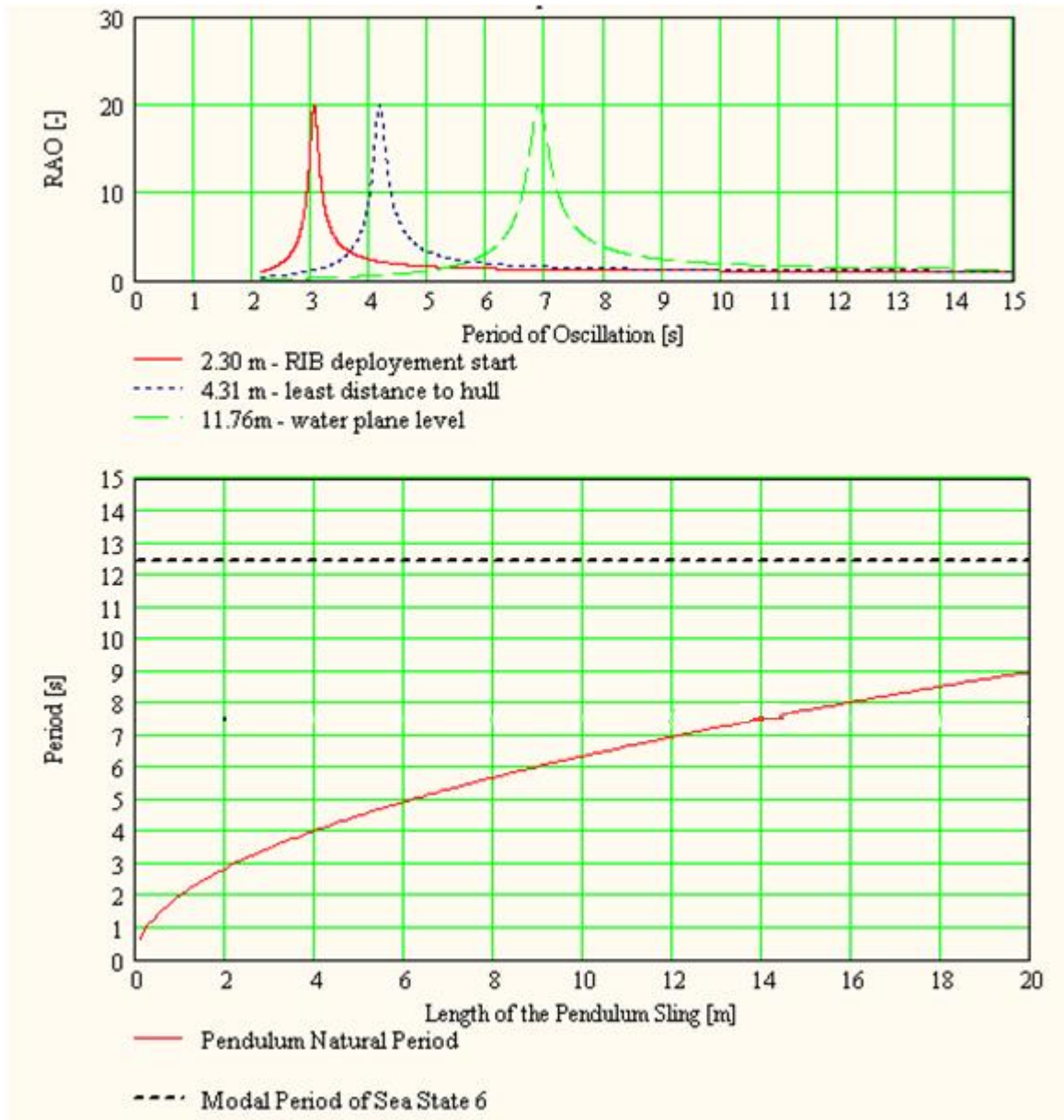


Figure 10 Pendulum response characteristics

Also, tests shown in Figure 11 and Figure 12 underline the effect of the continuous launch/recovery on the probabilities of failure when compared with stationary pendulation of the RIB. Allowing the RIB to oscillate, especially at its longest sling with RIB near the calm water level, leads to higher probabilities of failure than expected during prompt launch or recovery operation.

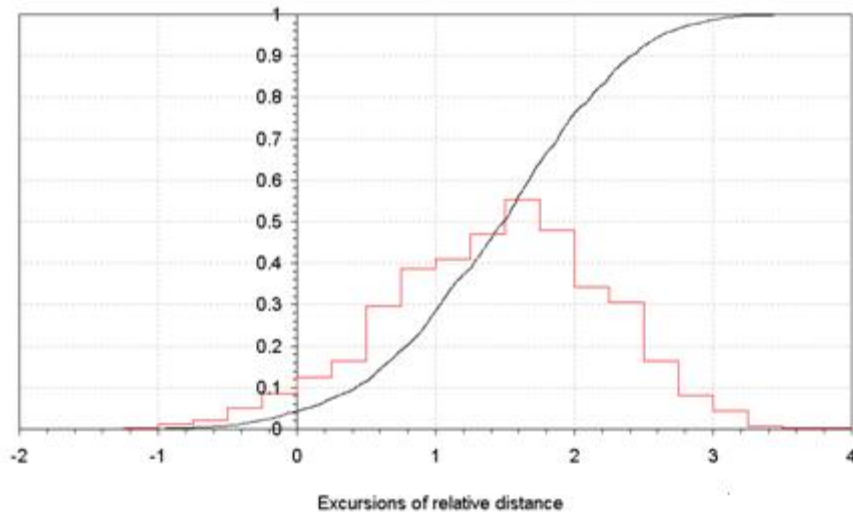


Figure 11 Statistics of the excursions of relative motion between sides of the RIB and the ship, assumed constant sling length of 11.16m

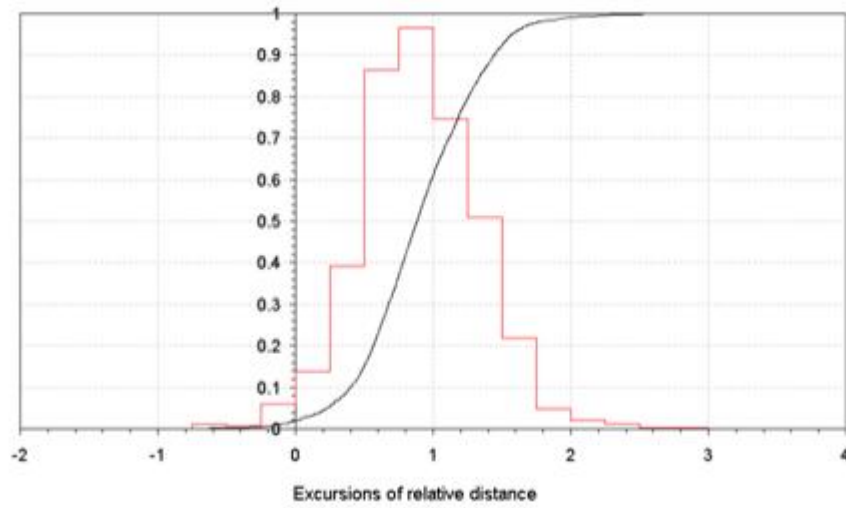


Figure 12 Statistics of the excursions of relative motion between sides of the RIB and the ship, assumed continuous operation of launch and recovery with sling length varying between 2.3 and 11.76m

APPENDIX 1 MATHEMATICAL BACKGROUND

Vessel response predictions

Equations describing ship behaviour (including damaged condition) are derived from fundamental motion principles: the law of conservation of linear and angular momentum. The law normally applied to rigid bodies, is here also extended to the internal fluid mass, resolved in a body-fixed system of reference, as shown in Figure 13. Rigorous derivation leads to a set of 6 scalar equations for linear and angular motions, as shown below.

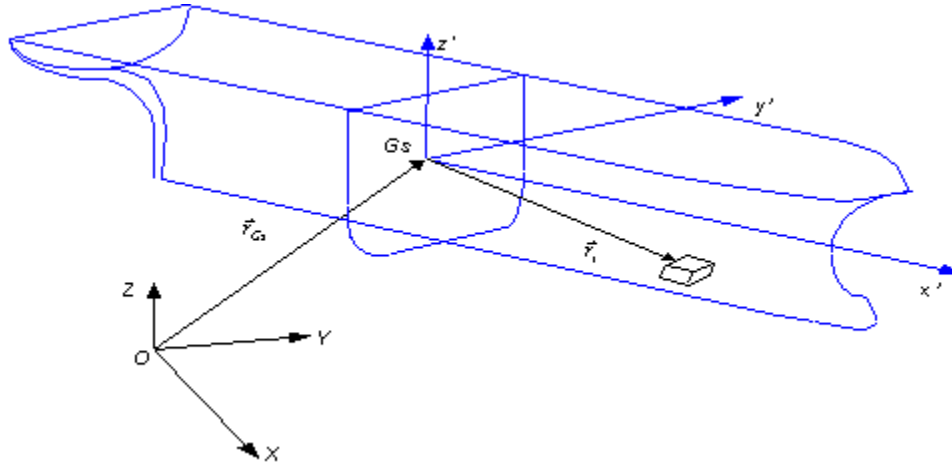


Figure 13: Coordinate system fixed to the centre of gravity of the intact vessel

$$\begin{aligned}
 & M_w \cdot \left[\frac{d}{dt} \vec{v}'_w + 2 \cdot \vec{\omega}' \times \vec{v}'_w + \frac{d}{dt} \vec{\omega}' \times \vec{r}'_w + \vec{\omega}' \times (\vec{\omega}' \times \vec{r}'_w) \right] + \\
 & + \frac{d}{dt} M_w \cdot (\vec{v}'_w + \vec{\omega}' \times \vec{r}'_w) + \\
 & + (M_s + M_w) \cdot \frac{d}{dt} \vec{v}'_s + \frac{d}{dt} M_w \cdot \vec{v}'_s + \vec{\omega}' \times (M_s + M_w) \cdot \vec{v}'_s = \vec{F}'
 \end{aligned} \tag{1}$$

$$\begin{aligned}
 & M_w \cdot \left[(\vec{\omega}' \times \vec{r}'_w) \times \vec{v}'_w + \vec{r}'_w \times \left[\frac{d}{dt} \vec{v}'_s + \frac{d}{dt} \vec{v}'_w + \vec{\omega}' \times (\vec{v}'_s + \vec{v}'_w) \right] \right] + \\
 & + \frac{d}{dt} M_w \cdot [\vec{r}'_w \times (\vec{v}'_s + \vec{v}'_w)] + \\
 & + (I'_s + I'_w) \cdot \frac{d}{dt} \vec{\omega}' + \left(\frac{d}{dt} I'_w \right) \cdot \vec{\omega}' + \vec{\omega}' \times [(I'_s + I'_w) \cdot \vec{\omega}'] = \vec{M}'_s
 \end{aligned} \tag{2}$$

The right hand side of the equation, \vec{M}'_s , and the respective force vector \vec{F}' of the rectilinear motions, represent all the external forces and moments acting on the vessel expressed in a body-fixed system of reference, G_s,xyz , located at the ship centre of mass. These forces/moments are predicted with conventional Naval Architecture methods. The Froude-Krylov and restoring forces and moments are integrated up to the instantaneous wave elevation, the radiation and diffraction forces and moments are derived from linear potential flow theory and expressed in time domain using convolution and spectral techniques, respectively. The hull asymmetry due to ship flooding, is

taken into account by a “database” approach, whereby the hydrodynamic coefficients are predicted beforehand, and then interpolated during the simulation.

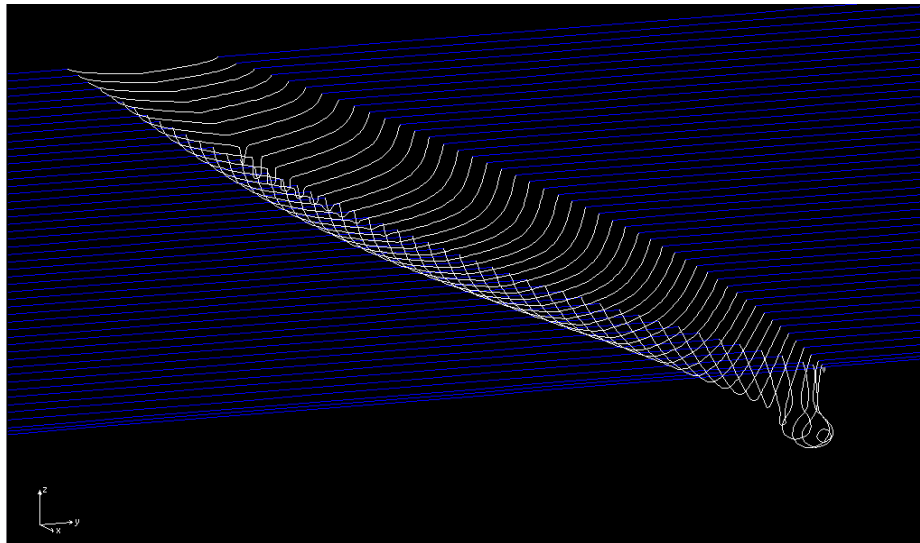


Figure 14 Vessels strips considered for predictions of vessel hydrodynamic properties

The second order drift forces, wind and current effects and other forces of viscous origin are also catered for, at present based on parametric formulations. Naturally the gravity force and moment vectors correspond to ship and floodwater weights.

$$\vec{F}'_s, \vec{M}'_s = \vec{F}'_{Gravity} + \vec{F}'_{F-K, Restoring} + \vec{F}'_{Radiation} + \vec{F}'_{Diffraction} + \vec{F}'_{Manoeuvring, Rudder} + \vec{F}'_{Drift, Current, Wind, Viscous}$$

Where:

$\vec{F}'_{Restoring}$ \vec{F}'_{F-K} Direct integration of static pressures on actual geometry

$\vec{F}'_{Radiation}$ Convolution techniques

$\vec{F}'_{Diffraction}$ Spectral techniques

$\vec{F}'_{Manoeuvring, Rudder}$ Empirical formulae

$\vec{F}'_{Drift, Current, Wind, Viscous}$ Empirical formulae

I'_s Inertia matrix of ship (“s”) w.r.t. G_s

I'_w Inertia matrix of water (“w”) w.r.t. G_s

$\vec{v}'_s, \vec{\omega}'$ Ship rectilinear and angular velocities

M_w Mass of floodwater in a single compartment

\vec{r}'_w Position vector of the centre of buoyancy of floodwater “w” in a body-fixed reference system with origin at G_s

\vec{v}'_w Velocity vector of the above point

| | |
|----------------|---|
| \vec{M}'_s | Resultant of all external moments acting on ship (three-component vector) |
| \vec{g}' | Gravity acceleration vector |
| $\frac{d}{dt}$ | Local time derivative |

A correction for viscous effects on roll motion is applied based on an established empirical method proposed in [3], where the viscous damping moment is divided into several components: friction, eddy shedding, lift, wave and bilge keel, and the total force is obtained by a superposition of all these components. However, the proposed method, representing the non-linear viscous damping as an equivalent linear coefficient at the roll natural frequency, remains a function of roll amplitude, which cannot be known *a priori* and hence not suitable for application to time-domain simulation in random seas. In this respect, an engineering approximation has been proposed in [4], whereby a discrete piece-wise constant treatment of the linearised coefficient is used with the coefficient evaluated at the wave spectrum peak frequency and for an amplitude corresponding to the amplitude of the last half-roll cycle. In this approach the viscous roll damping will vary with time, constantly adjusting to the current roll amplitude.

After re-arranging the whole system into a matrix form as a set of twelve differential equations of the first order, it is then solved for position in space of the centre of gravity of the intact ship $\vec{r}_{G_s} = \int \vec{v}_s \cdot dt$ and three rotations through a 4th order Runge-Kutta-Feldberg integration scheme with variable step size.

Coordinate systems

For proper interpretation of the numerical simulation results, it is necessary to clearly explain the space reference used. In this work five coordinate systems are employed for numerical description of ship motions, as explained below.

Earth-fixed, "inertial" reference frame $EX^E Y^E Z^E$ is assumed to delineate space. The $EX^E Y^E$ plane is fixed on the calm water level and the EZ^E axis points upwards, see Figure 15.

Ship motions can be decomposed into two components: steady and unsteady, the first denoting the ship moving forward with constant velocity at a given mean position and the second 6dof oscillations around her mean position. Following this, to simplify the motion description, a second inertial co-ordinate system OXYZ is adopted. The OXY plane is placed on the calm water level, and the OZ axis points upwards. The system moves with the mean, rectilinear motion of the ship, i.e. in case of no ship oscillations, the origin 'O' of the system is located at the intersection between water-plane, centre-line-plane and mid-ship-plane of the ship, see Figure 16. The OX axis points towards the bow of a ship and OY to port side. The angle between the EX^E and OX axes, β , defines the heading of the ship with respect to the oncoming waves, the propagation direction of which is assumed to be along the EX^E axis.

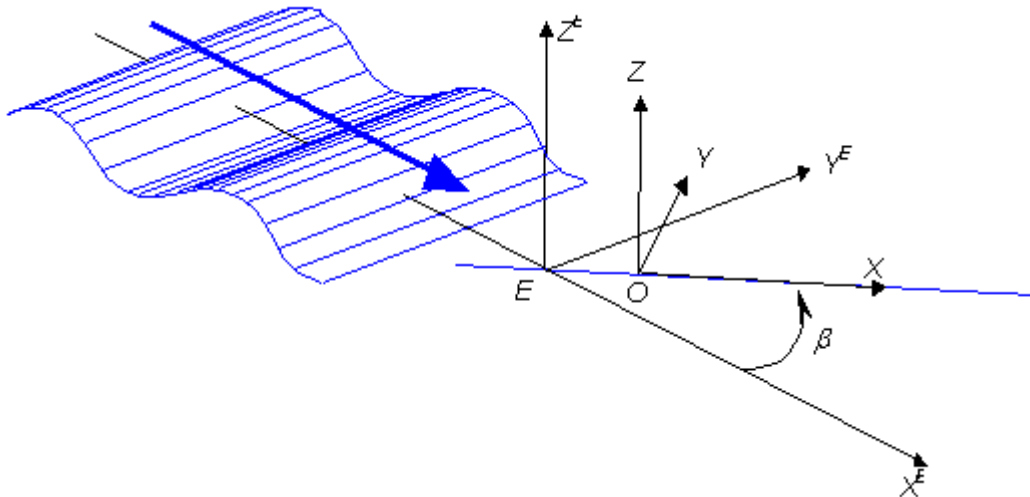


Figure 15 Definition of inertial co-ordinate systems

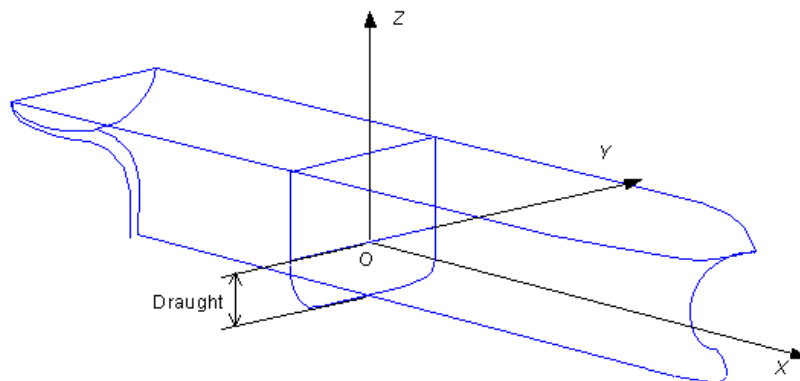


Figure 16 Inertial co-ordinate system in relation to ship with no oscillations

The ship-environment interaction will be expressed in the OXYZ co-ordinate system. Note here that the predicted vessel motions are expressed in the OXYZ coordinate system at its initial position ($t=0$), and for convenience this system will be referred to as $O^0X^0Y^0Z^0$.

Finally, the coordinate system Kxyz is employed for convenient description of the ship-related parameters: the geometry (*.G, *.SUS, *.DAM, etc), mass distribution, etc. Its origin is located at point K at the keel level, from intersection of three planes, the centre plane, midship section and base plane.

To summarise the coordinate systems are: $EX^EY^EZ^E$, (earth-fixed, wave description), OXYZ (mean ship speed-fixed, ship-environment interaction), $O^0X^0Y^0Z^0$, (earth-fixed, ship motion description), Axyz, (body-fixed, equations of motions solution), Kxyz (body-fixed, ship description).

RIB pendulation predictions

Vessel motions provide the excitation in the form of external acceleration to the RIB pendulum system. The pendulum is modelled as a driven spring-mass system as is shown below.

It is assumed that there is sufficient positive tension in the hoist wire such that the wire always remains completely straight.

$$(M \cdot l^2) \cdot \ddot{\alpha} = \vec{r}' \times \vec{F}' \quad \text{Equation of motion of the RIB due to pendulation, expressed in body-fixed system of reference} \quad (3)$$

Where:

$$\vec{r}' = l(t) \cdot \begin{bmatrix} 0 \\ \sin \alpha \\ -\cos \alpha \end{bmatrix} \quad \text{Vector of force action with respect to the attachment point } P \text{ of the RIB launching sling} \quad (4)$$

$$l(t) = v_l \cdot t \quad \text{Length of the launching sling} \quad (5)$$

$$v_l \quad \text{Launching speed of the RIB, [m/s]} \quad (6)$$

$$\vec{F}' = M \cdot (\vec{g}' - \vec{a}'_p) - \vec{F}'_{visc} \quad \text{Total external force vector acting on the mass } M \quad (7)$$

$$\vec{a}'_p = \vec{a}'_G + \frac{d\vec{\omega}}{dt} \times \vec{r}'_{GP} + \vec{\omega} \times (\vec{\omega} \times \vec{r}'_{GP}) \quad \text{Acceleration field at the attachment point } P \text{ of the RIB launching sling, due to ship motions} \quad (8)$$

$$\vec{r}'_{GP} \quad \text{Vector between centre of ship motions and the attachment point } P \text{ of the RIB launching sling} \quad (9)$$

$$\vec{\omega} = \omega'_x \cdot \vec{i}' + \omega'_y \cdot \vec{j}' + \omega'_z \cdot \vec{k}' \quad \text{Cartesian rotational velocity vector} \quad (10)$$

$$\vec{g}' = D \cdot \begin{bmatrix} 0 \\ 0 \\ -9.81 \end{bmatrix} \quad \text{Gravity acceleration field, [m/s}^2\text{], expressed in body fixed, non-inertial system of reference} \quad (11)$$

$$\vec{F}'_{visc} = \begin{bmatrix} 0 \\ \frac{1}{2} \cdot C_D \cdot \rho_{air} \cdot v^2 \cdot A_{pr} \\ 0 \end{bmatrix} \quad \text{Vector of drag forces acting on the RIB} \quad (12)$$

Rotation matrix between inertial and non-inertial coordinate systems:

$$D = \begin{bmatrix} \cos(\theta) \cdot \cos(\psi) & \cos(\theta) \cdot \sin(\psi) & -\sin(\theta) \\ \sin(\varphi) \cdot \sin(\theta) \cdot \cos(\psi) - \cos(\varphi) \cdot \sin(\psi) & \sin(\varphi) \cdot \sin(\theta) \cdot \sin(\psi) + \cos(\varphi) \cdot \cos(\psi) & \sin(\varphi) \cdot \cos(\theta) \\ \cos(\varphi) \cdot \sin(\theta) \cdot \cos(\psi) + \sin(\varphi) \cdot \sin(\psi) & \cos(\varphi) \cdot \sin(\theta) \cdot \sin(\psi) - \sin(\varphi) \cdot \cos(\psi) & \cos(\varphi) \cdot \cos(\theta) \end{bmatrix} \quad (13)$$

The typical free pendulation response is shown in Figure 18 below.

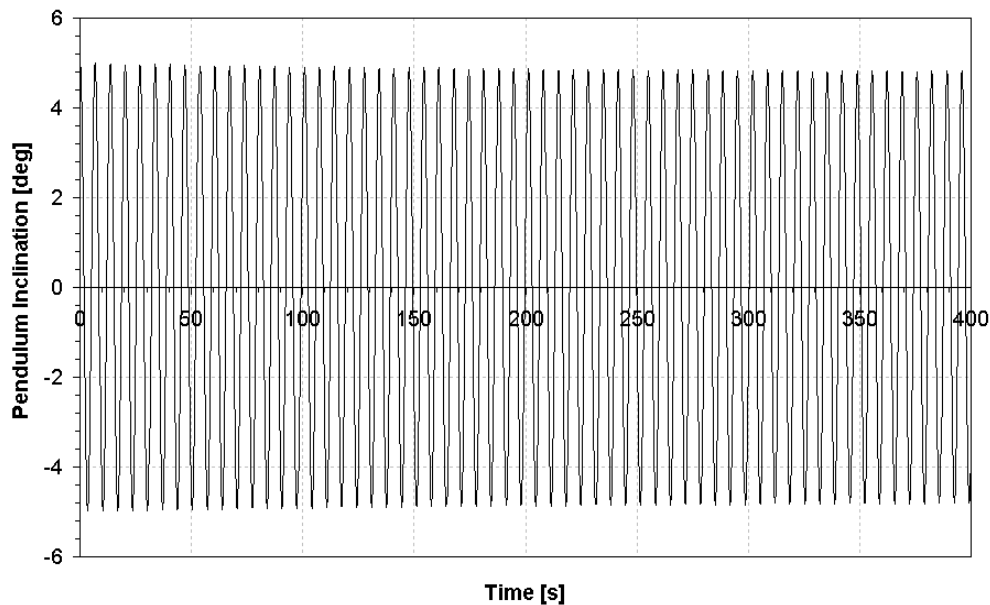


Figure 18 Free pendulation

The simulated response of the RIB in terms of its pendulation angles is given with respect to the ship-bound vertical axis. For instance if ship rolls to the starboard side with $\varphi = 10\text{deg}$ roll angle, the simulated pendulation will be $\alpha = -10\text{deg}$.

Literature

- [1] Cummins W.E., “*The impulse response function and ship motions*”, Schiffstechnik Bd. 9 – 1962.
- [2] Salvesen, N., Tuck, E.O. and Faltinsen, O.: “*Ship Motions and Sea Loads*”, SNAME, Vol. 78, 1970.
- [3] Himeno Y., “*Prediction of ship roll damping – state of the art*”, Report No 239, University of Michigan, College of Engineering, September 1981.
- [4] Jasionowski, A., “*An integrated approach to damage ship survivability assessment*”, PhD dissertation, February 2001, University of Strathclyde.

APPENDIX 2 ENVIRONMENT DESCRIPTION

Ambient waves on the surface of the ocean are random. The generating mechanism is, predominantly, the effect upon the water surface of wind in the atmosphere. There are at least two physical processes involved, namely the localised pressure fields and the friction between blown air and water. The wind is itself random, especially when viewed from the standpoint of the mentioned turbulent fluctuations and eddies. Additionally, the randomness of ocean waves is subsequently enhanced by their propagation over large distances in space and time and their exposure to the random non-uniformities of the water, seabed and air.

Although a great deal of work has been done on the theory of wave generation by wind, no completely satisfactory mechanism has yet been devised to explain the transfer of energy from wind to sea. However, advanced stochastic techniques have been devised to enhance and supplement physics-based analyses of ocean waves and their inherent power properties.

The profile of wind-generated waves observed in the ocean changes randomly with time and in space, and it is non-repeatable in neither of these domains. In reality, both wave height and wave period vary randomly from one cycle to another. If thus randomly changing waves are considered as a stochastic process, then it is possible to evaluate the statistical properties of waves through the frequency and probability domains. In the stochastic process approach, waves in deep water are categorised as (a) steady state ergodic random process and (b) a Gaussian random process for which the probability of displacements from the mean value (wave profile) obeys the normal probability law. This rationale forms a basis for mathematical representation of random ocean time and space wave profiles as superposition of infinite number of sine waves of different height, frequency and direction.

In this approach, proposed by St Denis and Pierson in 1953, the amplitudes of the individual wave components are expressed in terms of a function known as a variance spectrum. The variance spectrum, more often referred to as a point spectrum has evolved over years as the most common technique to provide with measure of severity of any sea. If the wave point spectrum is assumed narrow-banded, which is valid assumption for most of ocean waves, it is a source of practically derivable information from which the above mentioned time series composition as well as probabilistic prediction of various wave properties can be obtained in the probability domain.

Note that because the variance of individual wave components also corresponds to their energy, the point spectrum is often called, somewhat loosely, the wave energy spectrum.

The shape of wave spectra varies considerably, depending on the severity of wind velocity, time duration of wind blowing, fetch length, etc. Many spectral formulations have been proposed since early 1950. Widely used formulation is the so called JONSWAP point spectrum, derived from extensive wave measurement program known as Joint North Sea Wave Project carried out in 1968 and 1969 along a line extending over 160 km into the North Sea from Sylt Island. The spectrum represents wind-generated seas with fetch limitation.

The JONSWAP wave variance spectrum has been used in this project to describe the environment (sea). Its formulation is given by (14):

$$S(\omega) = \frac{0.0624}{0.23 + 0.0336 \cdot \gamma - \frac{0.185}{1.9 + \gamma}} \cdot H_s^2 \cdot \frac{\omega^{-5}}{\omega_p^{-4}} \cdot e^{-\frac{5}{4} \left(\frac{\omega_p}{\omega} \right)^4} \cdot \gamma \frac{(\omega - \omega_p)^2}{2\tau^2 \cdot \omega_p^2} \quad (14)$$

Where:

$$\tau = \begin{cases} 0.09 & \text{if } \omega > \omega_p \\ 0.07 & \text{if } \omega \leq \omega_p \end{cases} \quad (15)$$

$$\gamma = 1 \quad \text{Peakness parameter} \quad (16)$$

$$H_s \quad \text{Significant wave height} \quad (17)$$

$$\omega_p \quad \text{Modal frequency} \quad (18)$$

The sample wave elevation histories in time and space domains, generated based on (14), are shown in Figure 19 to Figure 21 below.

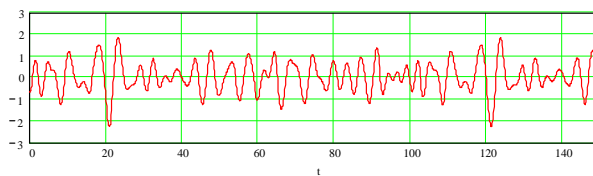


Figure 19 Time domain long-crested wave realisation of ζ at one point $x=y=0m$.

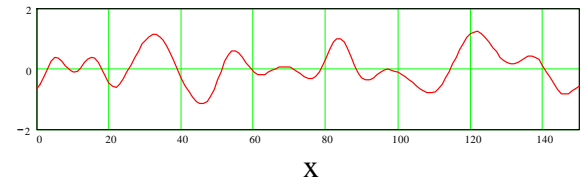


Figure 20 Space-wise long-crested wave realisation of ζ for $t=0s$.

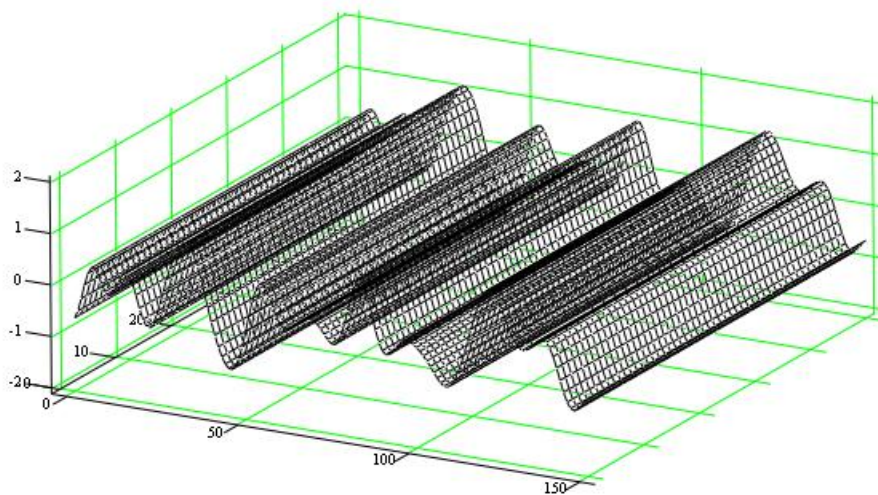


Figure 21 A 3D view of the sample space-wise realisation of long-crested wave profile for $H_s=2.0$ m, and $T_p=5.6$ s, $t=0$ s.

B. APPENDIX B

This annex describes the calculations done in order to evaluate the probability of injuries when the lifeboat hits the water during lowering.

Model

The lifeboat considered for this study is a 150 person standard one, with the following main characteristics:

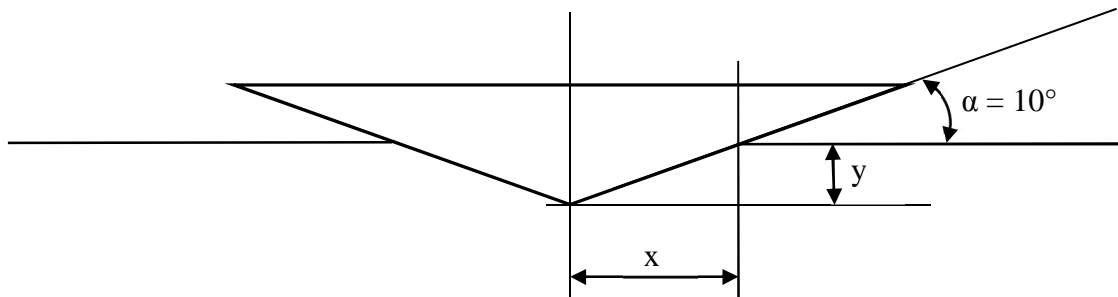
| Length (m) | Breadth (m) | Height to gunwale (m) | Weight w/o persons (kg) |
|------------|-------------|-----------------------|-------------------------|
| 9.6 | 4.3 | 1.9 | 5700 |

The bottom of the lifeboat is wedge shaped except for the keel. (von Karman, 1929) derived the impact formula for a two dimensional wedge shape. The bottom of the lifeboat is therefore simplified to a wedge shape, without keel. This will give an over prediction of the accelerations, since the keel will already split the water. The von Karman approach gives an under prediction of the actual slamming accelerations, so a simplification to a wedge will give a good indication of the accelerations. Figure 22 shows the wedge model used in the von Karman approach.

In the von Karman approach the weight of the boat per unit length is needed. The empty weight of the boat is equal to 5700 kg. The boat can accommodate a maximum of 150 passengers, with an average weight of 75 kg. This leads to a total weight of approximately 17 tons. To take into account the different shape of the front and aft of the boat, the length of the boat over which the total weight is distributed is a little less than the overall length of the boat and is estimated to be equal to 8 m. This leads to a mass per unit length of 2,125 tons, and a weight of 20.846 kN/m. The deadrise, α , of the bottom is measured from the lifeboat drawing to be equal to 10 degrees.

The wedge in the von Karman approach is rigid. In reality the lifeboat has some flexibility and also the accelerations 'felt' by the bottom of the lifeboat may differ somewhat from the accelerations felt by the passengers. However, the approach gives a good indication of the order of magnitude of the accelerations felt by passengers of the lifeboat.

Figure 22 - Wedge model of lifeboat bottom



Von Karman impact formula

In his paper, von Karman determined the vertical speed and accelerations of the wedge as a function of the horizontal breadth of the body in the water.

$$v_{vert} = \frac{\partial y}{\partial t} = \frac{v_0}{1 + \frac{\rho g \pi x^2}{2W}}$$

$$a_{vert} = \frac{\partial^2 y}{\partial t^2} = \frac{-v_0^2}{\left(1 + \frac{\rho g \pi x^2}{2W}\right)^3} \times \frac{\rho g \pi x}{W \cdot \tan(\alpha)}$$

In which:

v_{vert} = vertical speed [m/s]

a_{vert} = vertical accelerations [m/s²]

x = half of breadth of body in water [m] (see Figure 22)

y = submerged depth [m] (see Figure 22)

$g = 9.81$ = Gravity load [m/s²]

$\alpha = 10^\circ$ = Deadrise angle

$W = 20846$ = Boat weight per unit length [N/m]

$\rho = 1030$ = Water density [kg/m³]

h = Drop height [m]

v_0 = Velocity of the boat at first impact [m/s]

The velocity of the boat at first impact is determined in following paragraphs.

Time can be estimated using:

$$\partial t(x) = \frac{\partial y(x)}{v_{vert}(x)} \approx \frac{\Delta y(x)}{v_{vert}(x)}$$

Velocity of the boat at first impact

Scenario 1

The lifeboat is lowered at normal speed and hits the moving water surface.

Wave and ship movements

Previous hydrodynamic calculations on a large cruise vessel give the lifeboat vertical relative velocity. Calculations were done with no lifeboat lowering speed.

Figure 23 - Lifeboat relative velocity

| Scenario | Sea State | Heading angle (°) | Life boat relative velocity | | | | | |
|----------|-----------|----------------------|-----------------------------|--------------|--------------------|----------------------|----------------------|-----------|
| | | | Side | RMS (m/s) | $A_{1/3}$ (m/s) | $A_{1/100}$ (m/s) | A_{max6h} (m/s) | T2 (s) |
| 2 | 3 | 90 | Leeward | 0.24 | 0.29 | 0.69 | 1.01 | 3.79 |
| | | | Windward | 0.30 | 0.34 | 0.85 | 1.26 | 4.37 |
| 3 | 5 | 180 | Leeward | 0.73 | 0.79 | 2.06 | 3.08 | 4.81 |
| | | | Windward | 0.73 | 0.79 | 2.06 | 3.08 | 4.81 |
| 4 | 5 | 90 | Leeward | 0.67 | 0.75 | 1.91 | 2.84 | 4.48 |
| | | | Windward | 0.88 | 0.96 | 2.50 | 3.71 | 5.20 |
| 5 | 6 | 90 | Leeward | 0.78 | 0.81 | 2.19 | 3.28 | 5.25 |
| | | | Windward | 1.00 | 1.06 | 2.84 | 4.21 | 5.86 |

Probability

The velocity at the moment of impact can be considered to be taken randomly and the velocity distribution then follows a Gauss distribution:

$$P_{Gauss}(v) = \Phi\left(2 \frac{v}{v_{rel}}\right)$$

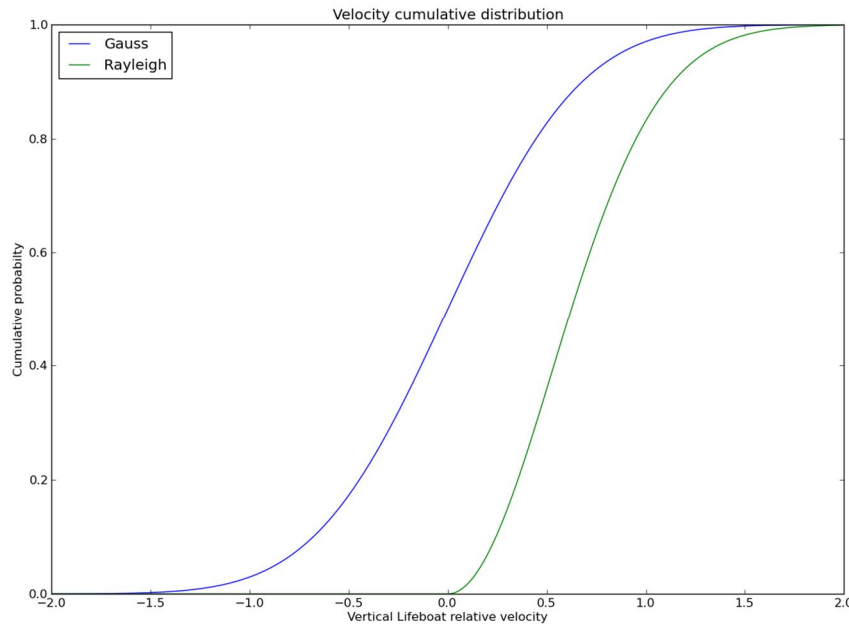
Where v_{rel} is the single amplitude significant velocity, here equal to $A_{1/3}$.

The velocity distribution can also be considered as close to the distribution of the velocity maxima:

$$P_{Rayleigh}(v) = 1 - e^{-2\left(\frac{v}{v_{rel}}\right)^2}$$

Where v_{rel} is the single amplitude significant velocity, here equal to $A_{1/3}$.

Figure 24 - Velocity cumulative distribution – example for $v_{rel} = A_{1/3} = 1.06$ (Sea State 6 – Windward, worstcase)



As expected the Rayleigh distribution is more conservative.

Lowering speed

The lowering speed according to LSA Code (2003, 6.1.2.8) should be not less than:

$$S = 0.4 + 0.02H$$

Where:

S is the lowering speed in metres per second and

H is the height in metres from the davit head to the waterline with the ship in the lightest sea-going conditions.

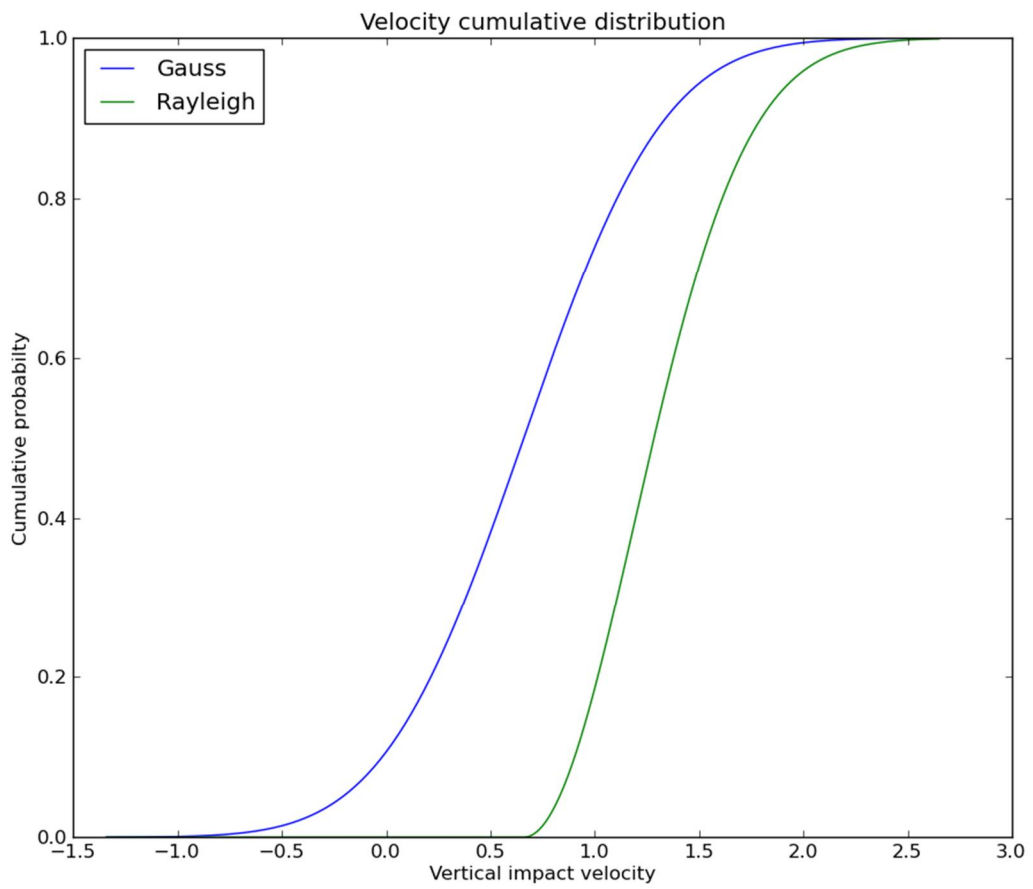
In the present case, $H \approx 13$ m ; $S \approx 0.66$ m/s

Impact speed

The impact speed is the sum of relative velocity and lowering speed. So v_0 follows the following distribution:

$$P_{Rayleigh}(v_0) = 1.66 - e^{-2\left(\frac{v_0}{A_{1/3}}\right)^2}$$

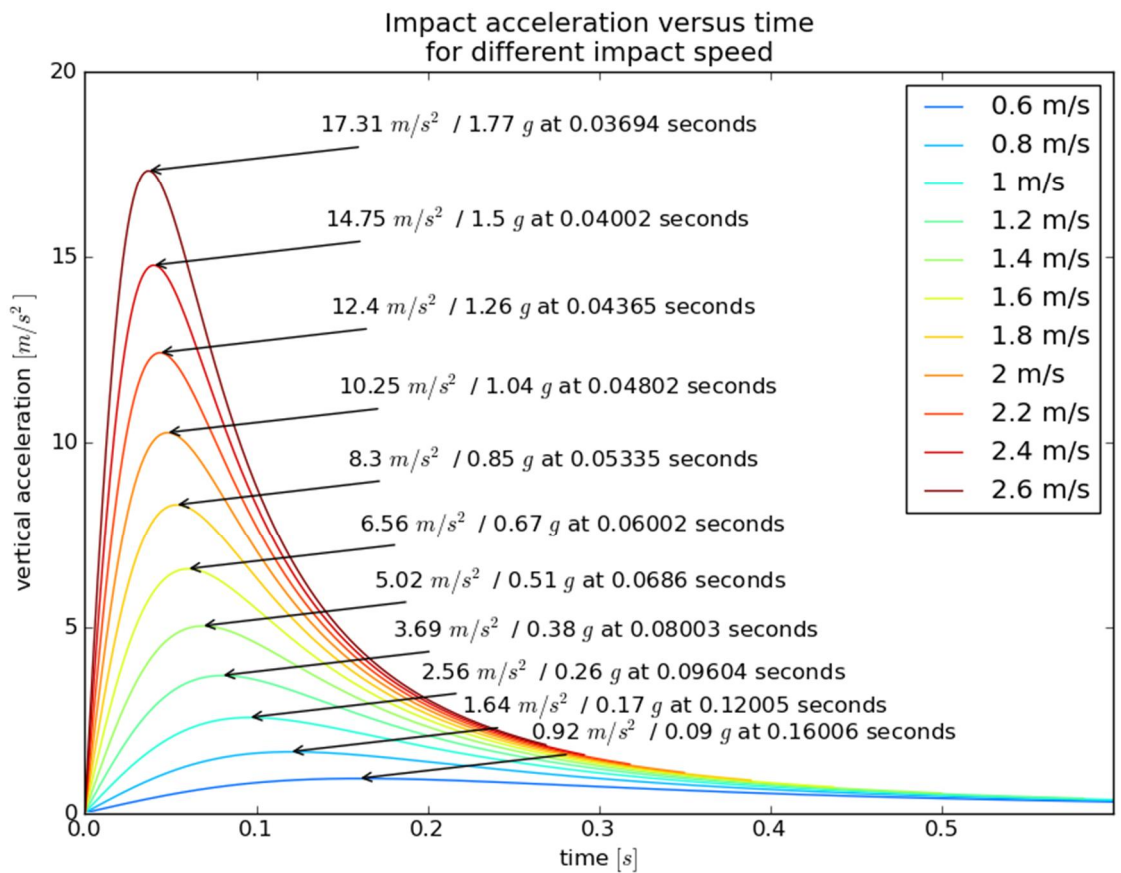
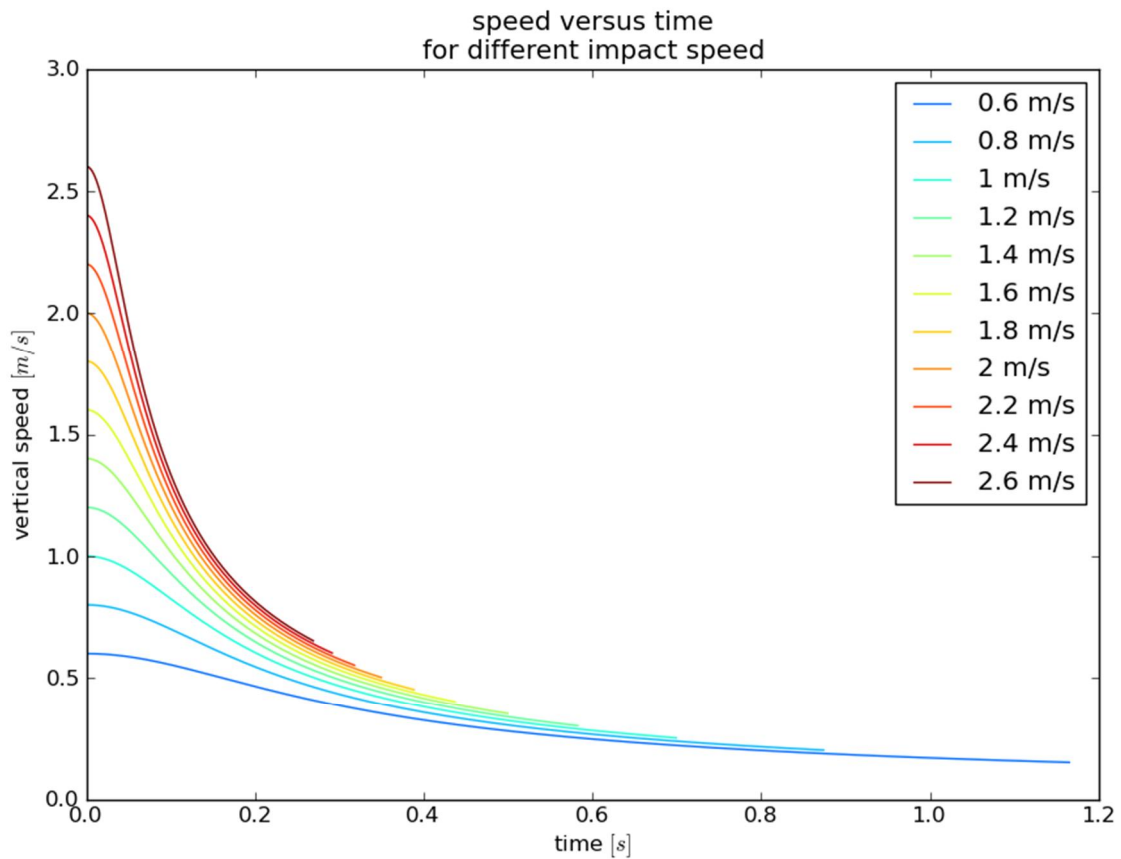
Figure 25 – Impact speed cumulative distribution – exemple for $v_{rel} = A_{1/3} = 1.06$ (Sea State 6 – Windward, worstcase)



Results

Figure 26 gives the lifeboat speed and acceleration versus time for different impact speeds.

Figure 26 - Graphs showing speed and acceleration versus time



Scenario 2

This scenario corresponds to a drop of the lifeboat if not released on a wave crest. The velocity of the boat at first impact depends on the drop height of the boat:

$$v_0 = \sqrt{2gh}$$

This is the scenario that was used in the Safecrafts project.

Probability

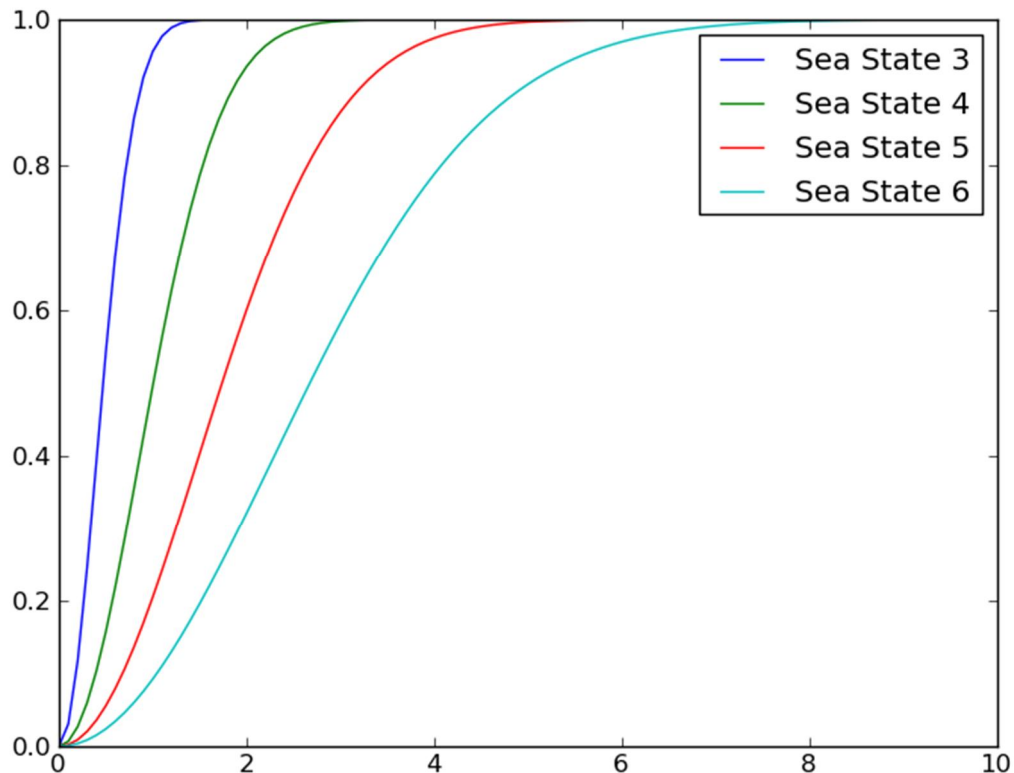
In a moderate gale (Sea state 6, H_s 4 to 6 m), it is assumed that the probability of occurrence of 6 m drop height is 25%; the probability of 2 m drop height is 25%; and the probability of no drop at all is 50%.

The wave height distribution (peak-to-through wave height) can be described as a Rayleigh distribution:

$$P_{WaveHeightCumul}(h) = e^{-\left(\frac{h}{\alpha_H \cdot H_s}\right)^2}$$

With $\alpha_H = \frac{1}{2}\sqrt{1-\rho}$ and $\rho = -0.65$

Figure 27 - Cumulative distribution of peak-to-through wave height



So probability of a wave being higher than 2 m is

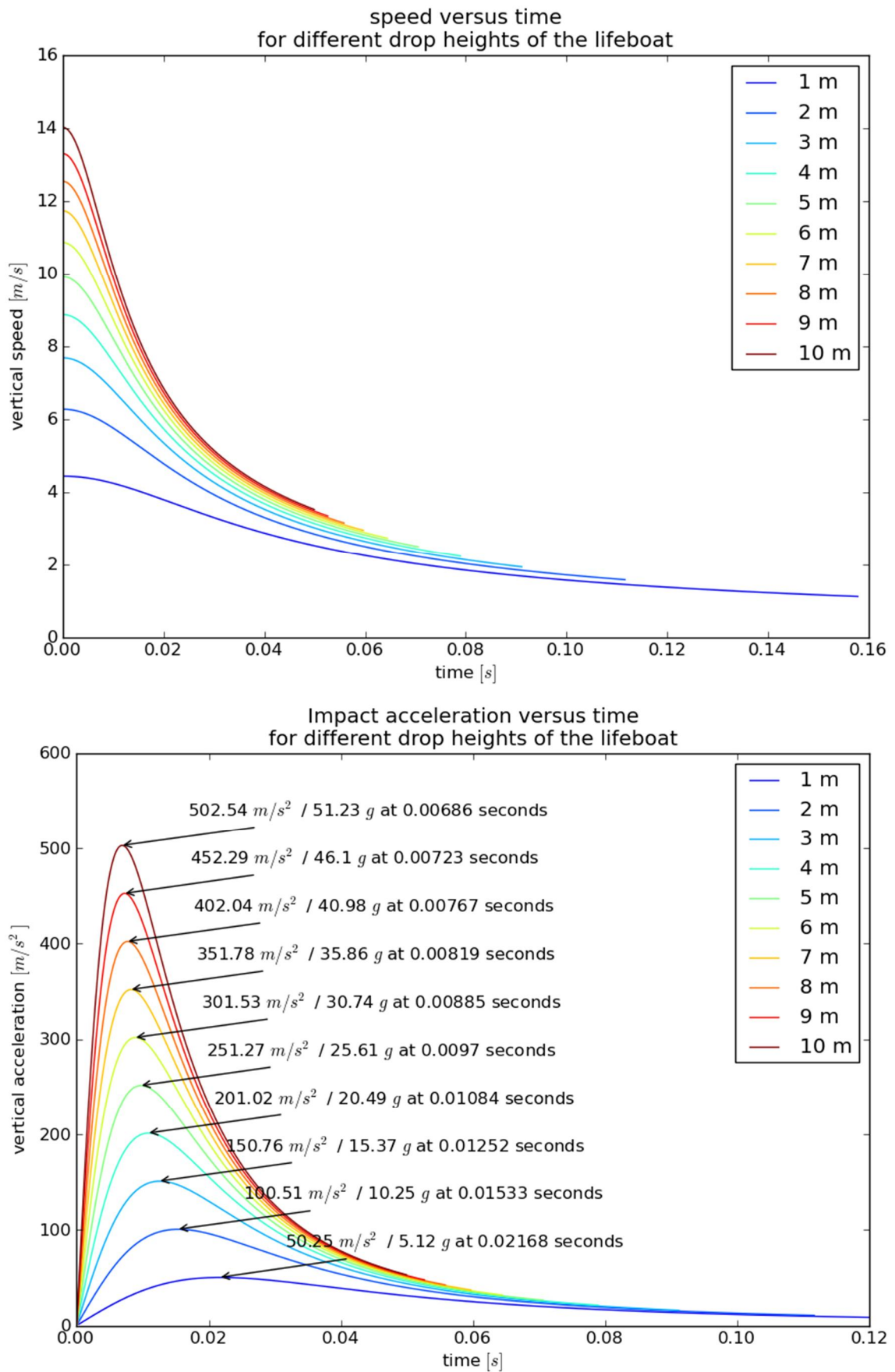
$$P(h > 2m) = 1 - P_{WaveHeightCumul}(2)$$

In calm weather (Sea State 3), no slamming is to be expected ($P(h > 2m) = 3.6 \times 10^{-6}$).

Results

Figure 28 gives the speed and acceleration versus time for different drop heights.

Figure 28 - Graphs showing speed and acceleration versus time



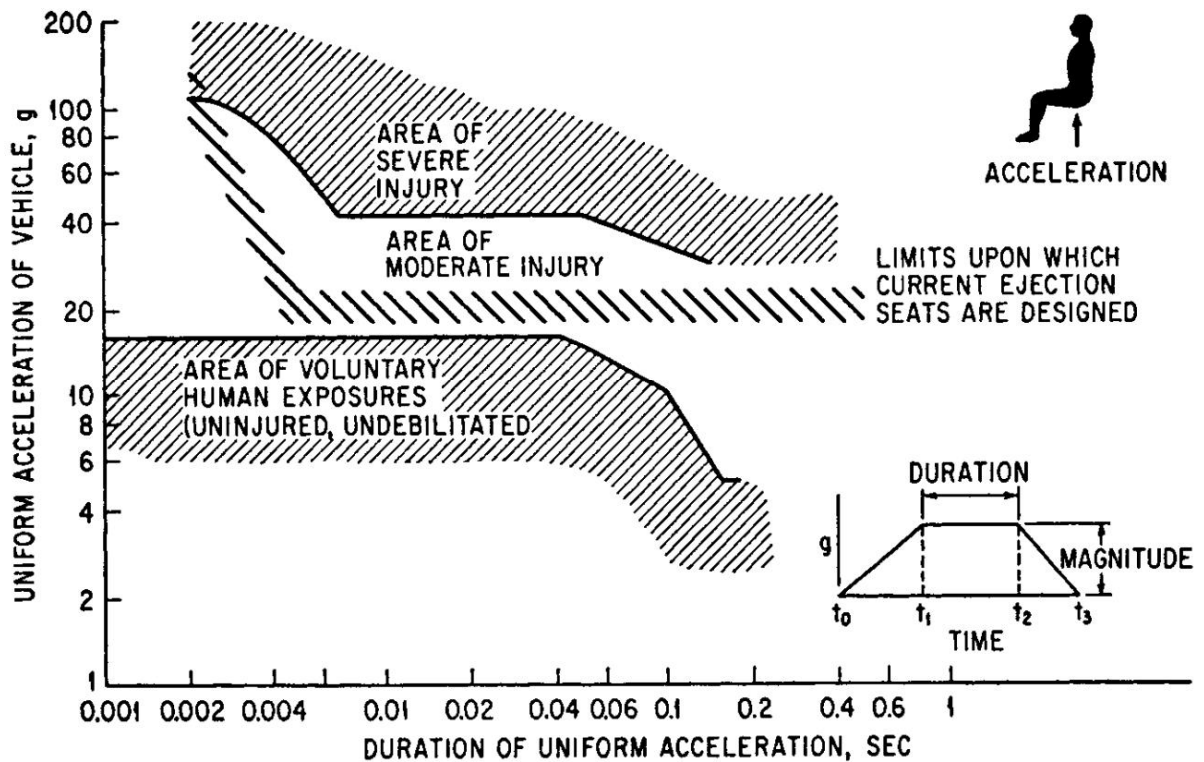
Effect on human health

Figure 29 (Harris & Bert, 2002) shows the effect of vertical acceleration on human health, it may be simplified as followed (this is true for an impact duration from 0.007s to 0.04s): people are uninjured until 16 g, moderately injured until 43g, and severely injured above this threshold.

First scenario: Figure 26 shows that acceleration is very low (below 2g) so no injuries are expected.

Second scenario: Figure 28 shows that accelerations cross the 43g barrier, so severe injuries are expected above a drop height of 8 m. For drop heights below 2 m, no injuries are expected. From 3 m to 8 m drop heights, moderate injuries are expected.

Figure 29 - Effect of vertical acceleration on human health (Harris & Bert, 2002)



Those values are for a young healthy subject with a safety belt. Older people will sustain less acceleration.

The following limits will be considered:

| | Moderate injuries | | Severe injuries | |
|-----------------------------|---------------------|-------------|---------------------|-------------|
| | Impact acceleration | drop height | Impact acceleration | drop height |
| Less than 50 years old | 16g to 43g | 3 m to 8 m | Above 43g | Above 8 m |
| Between 50 and 75 years old | 12g to 32g (-25%) | 2 m to 7 m | Above 35g | Above 7 m |
| Above 75 years | 10g to 26g (-40%) | 2 m to 5 m | Above 26g | Above 5 m |

Obstacle matrix

Using the probability defined in the 2nd scenario, applied to the effect on human health, the following obstacle matrix can be defined:

Sea state 1 to 3, all age categories:

| | GH | MI | SI | D |
|----|----|----|----|---|
| GH | 1 | 0 | 0 | 0 |
| MI | 0 | 1 | 0 | 0 |
| SI | 0 | 0 | 1 | 0 |
| D | 0 | 0 | 0 | 1 |

Sea state 4:

| <50 | GH | MI | SI | D |
|-----|--------|----|----|---|
| GH | 0.9980 | 0 | 0 | 0 |
| MI | 0.0020 | 1 | 0 | 0 |
| SI | 0 | 0 | 1 | 0 |
| D | 0 | 0 | 0 | 1 |

| 50-75 | GH | MI | SI | D |
|-------|--------|----|----|---|
| GH | 0.9940 | 0 | 0 | 0 |
| MI | 0.0060 | 1 | 0 | 0 |
| SI | 0 | 0 | 1 | 0 |
| D | 0 | 0 | 0 | 1 |

| >75 | GH | MI | SI | D |
|-----|--------|----|----|---|
| GH | 0.9936 | 0 | 0 | 0 |
| MI | 0.0064 | 1 | 0 | 0 |
| SI | 0 | 0 | 1 | 0 |
| D | 0 | 0 | 0 | 1 |

Sea state 5:

| <50 | GH | MI | SI | D |
|-----|--------|----|----|---|
| GH | 0.8740 | 0 | 0 | 0 |
| MI | 0.1260 | 1 | 0 | 0 |
| SI | 0 | 0 | 1 | 0 |
| D | 0 | 0 | 0 | 1 |

| 50-75 | GH | MI | SI | D |
|-------|--------|----|----|---|
| GH | 0.6010 | 0 | 0 | 0 |
| MI | 0.3990 | 1 | 0 | 0 |
| SI | 0 | 0 | 1 | 0 |
| D | 0 | 0 | 0 | 1 |

| >75 | GH | MI | SI | D |
|-----|--------|--------|--------|---|
| GH | 0.6005 | 0 | 0 | 0 |
| MI | 0.3960 | 0.9956 | 0 | 0 |
| SI | 0.0032 | 0.0040 | 0.9992 | 0 |
| D | 0.0003 | 0.0004 | 0.0008 | 1 |

Sea state 6:

| <50 | GH | MI | SI | D |
|-----|--------|--------|--------|---|
| GH | 0.5818 | 0 | 0 | 0 |
| MI | 0.4160 | 0.9973 | 0 | 0 |
| SI | 0.0020 | 0.0025 | 0.9995 | 0 |
| D | 0.0002 | 0.0002 | 0.0005 | 1 |

| 50-75 | GH | MI | SI | D |
|-------|--------|--------|--------|---|
| GH | 0.3205 | 0 | 0 | 0 |
| MI | 0.6700 | 0.9883 | 0 | 0 |
| SI | 0.0086 | 0.0107 | 0.9979 | 0 |
| D | 0.0009 | 0.0011 | 0.0021 | 1 |

| >75 | GH | MI | SI | D |
|-----|--------|--------|--------|---|
| GH | 0.3144 | 0 | 0 | 0 |
| MI | 0.5890 | 0.8892 | 0 | 0 |
| SI | 0.0885 | 0.1008 | 0.9802 | 0 |
| D | 0.0081 | 0.0100 | 0.0198 | 1 |

References

Harris, C. M., & Bert, C. W. (2002). *Shock and Vibration Handbook (5th ed.)*.
Journal of Applied Mechanics.

von Karman, T. (1929). *The Impact on Seaplane floats during landing*.